

# Chapter 4

## Compaction, Permeability and Flow Simulation for Liquid Composite Moulding of Natural Fibre Composites

Darshil U. Shah and Mike J. Clifford

**Abstract** With the growing interest in developing high-performance natural fibre composites (NFRPs) for (semi-)structural applications, researchers are increasingly considering liquid composite moulding (LCM) processes and investigating key manufacturing-related issues. Here, we critically review the literature on LCM of NFRPs. Consequently, we identify key findings concerning the reinforcement-related factors (namely, compaction and permeability) that influence, if not govern, the mould-filling stage during LCM of NFRPs. In particular, the differences in structure (physical and chemical) of natural and synthetic fibres, their semi-products (i.e. yarns and rovings) and their textiles are shown to have a perceptible effect on their processing via LCM.

**Keywords** Polymer-matrix composites • Liquid composite moulding • Resin transfer moulding • Compaction • Permeability • Flow modelling • Natural fibres • Biocomposites

---

D.U. Shah (✉)

Oxford Silk Group, Department of Zoology, University of Oxford,  
South Parks Road, Oxford OX1 3PS, UK

Department of Architecture, University of Cambridge, Cambridge CB2 1PX, UK  
e-mail: [dus20@cam.ac.uk](mailto:dus20@cam.ac.uk); [darshil.shah@hotmail.co.uk](mailto:darshil.shah@hotmail.co.uk)

M.J. Clifford

Polymer Composites Research Group, Division of Materials, Mechanics and Structures,  
Faculty of Engineering, The University of Nottingham, Nottingham NG7 2RD, UK

## 4.1 Introduction

### 4.1.1 *Liquid Composite Moulding*


It is estimated that in 2011, liquid composite moulding (LCM) accounted for 4 % (ca. 350 kilotonnes) of the global (Reux 2012) and 11 % (ca. 120 kilotonnes) of the EU (Witten and Jahn 2013) fibre-reinforced plastics' (FRPs) production volume. Notably, the use of LCM has grown consistently over the last few decades, particularly because they require low capital investment and are closed-mould processes offering better working conditions (viz., health and safety) and enhanced part quality (viz., mechanical properties, defects and surface finish) than open-mould processes. In general, LCM is primarily used for the cost-effective production of high-performance components with moderate-to-high complexity geometry and moderate-to-large size (up to 100 m<sup>2</sup>) at low-to-medium volumes (e.g. 100–10,000 parts/year): from automotive parts to wind turbine blades (Manson et al. 2000).

With the increasing usage of LCM, numerous process variants have evolved with resin transfer moulding (RTM), vacuum-assisted RTM and light RTM being the most commonly used (Campbell 2003; Long et al. 2005). In general, an LCM process can be divided into four stages (Table 4.1): (1) reinforcement layup, (2) mould filling, (3) post-filling and (4) demoulding. The basic approach in any LCM process is to force a catalysed thermosetting liquid resin to flow through a dry, stationary, porous, compacted reinforcement inside a closed mould by creating a pressure differential between the inlet(s) and outlet(s).

As the primary aim of any LCM process is to ensure complete filling of the mould, successful execution of LCM involves understanding, controlling and optimising the mould-filling stage in particular. This stage dictates the production cycle time, quality (viz., defects including voids and dry spots), geometry (e.g. thickness) and, ultimately, mechanical properties of the final part (Table 4.1). Not surprisingly, computational mould-filling simulations are widely used as a cost-efficient and time-saving tool to optimise the LCM process (Long et al. 2005). However, accurate manufacturing process simulations require accurate input data. Notably, the principal reinforcement-related factors affecting the mould-filling stage are compaction and permeability (Table 4.1).

In this chapter, we examine the processing of natural fibre-reinforced plastics (NFRPs) via LCM. We specifically inspect the through-thickness compaction behaviour and permeability of natural fibre reinforcements and highlight their key differences from synthetic fibre reinforcements. These insights are then used as foundations to discuss the modelling of the mould-filling stage in LCM of natural fibre reinforcements using adapted resin flow models.

**Table 4.1** Schematic and description of a generic LCM process illustrating the four principal stages

Stage	1. Reinforcement layup	2. Mould filling	3. Post-filling	4. Demoulding
<p><b>Schematic</b></p> 	<p>Layup of the dry reinforcement (multiple layers of textiles or a prefabricated 'preform') in a mould with a rigid (metal) or semi-rigid (composite) bottom tool and a rigid (metal), semi-rigid (composite) or flexible (silicone membrane or vacuum bag film) top tool/surface</p> <p>(a) Tool: design (incl. geometry) and material            (b) Reinforcement: layup (incl. type, architecture, number of layers, orientation)</p>	<p>'Dry compaction' of the reinforcement, followed by resin impregnation via drawing vacuum and/or injecting resin under pressure</p> <p>(a) Tool: design (incl. geometry, inlet/outlet gate location)            (b) Reinforcement: layup, compaction, permeability            (c) Resin: temperature, viscosity, degree of cure (all a function of time)            (d) Pressure differential in mould cavity, tooling temperature</p>	<p>'Wet compaction' of the impregnated reinforcement to allow laminate thickness to equilibrate, followed by curing of resin, possibly at elevated temperatures</p> <p>(a) Reinforcement: 'wet' compaction and permeability            (b) Resin: cure kinetics            (c) Heat transfer, pressure differential in mould cavity, tooling temperature</p>	<p>Demoulding of the cured, stiff composite part</p> <p>(a) Tool: geometry, surface release properties            (b) Resin: cure kinetics</p>
<p><b>Factors affecting this stage</b></p>	<p>(a) Cycle time (layup time)            (b) Part quality: layup-related defects (e.g. fibre/ply misalignment, incorrect fibre content distribution, mould closure problems)            (c) Part mechanical properties (incl. fibre volume fraction)</p>	<p>(a) Cycle time (fill time)            (b) Part quality: infusion-related defects (e.g. voids/porosity, dry spots, fibre/ply washing and misalignment), part geometry (incl. thickness)            (c) Part mechanical properties (incl. fibre volume fraction)</p>	<p>(a) Cycle time (post-fill time)            (b) Part quality: cure-related defects (e.g. incomplete cure, ply cracking, warpage), part geometry (incl. thickness) and tolerances            (c) Part mechanical properties (incl. fibre volume fraction)</p>	<p>(a) Part quality: surface finish, defects (e.g. print through, warpage, spring in, delamination), part geometry (incl. thickness) and tolerances            (b) Part mechanical properties</p>
<p><b>Factors affected by this stage</b></p>	<p>Process variations primarily relate to the choice of mould material and the resin injection/infusion mechanism</p>			

### 4.1.2 Natural Fibre Composites in LCM Processes

NFRPs accounted for over 13 % of the 2.4 million tonne EU FRP market in 2010 (Fig. 4.1) (Carus 2011; Carus and Gahle 2008; Shah et al. 2013a, b). While wood and cotton were used as reinforcements in the majority of these NFRPs [most likely due to their wide availability and low cost (Shah 2013b)], even the production of non-wood, non-cotton, plant fibre (e.g. flax, jute, hemp)-reinforced plastics (PFRPs) was comparable to the production of non-glass, synthetic fibre (e.g. carbon, aramid) composites.

The increasing consideration of natural fibres as next-generation, sustainable reinforcements requires tackling the first hurdle, which is composite manufacture [reviewed in (Pickering 2008; Summerscales et al. 2010; Faruk et al. 2012; Ho et al. 2012; Shah 2013b)]. Due to the commercial applications of NFRPs in predominantly small-sized, high-volume, low-cycle time, nonstructural components (e.g. decking for construction industry and interior panels for automotive industry), injection/extrusion moulding and compression moulding are the widely used manufacturing techniques (Fig. 4.1) (Shah 2013b; Carus et al. 2014). The reinforcement form has typically been pellets/granules for the former and random fibre mats for the latter. While wood and cotton reinforced NFRPs largely (>80 %) employ thermosetting matrices, PFRPs are primarily (>70 %) based on thermoplastic matrices (Fig. 4.1) (Carus and Gahle 2008; Shah 2013b; Carus et al. 2014).

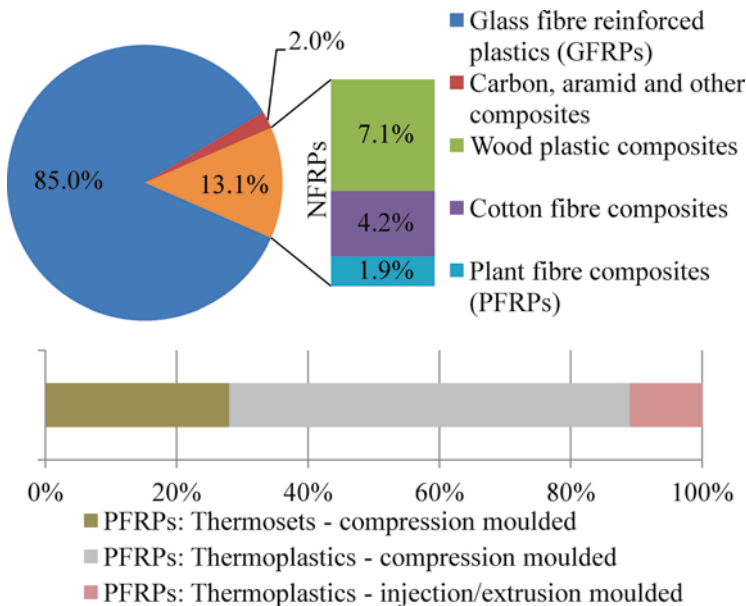


**Fig. 4.1** The production of NFRPs in the 2.4 million tonne EU FRP market in 2010 (Carus 2011; Carus and Gahle 2008; Shah et al. 2013a, b)

LCM, on the other hand, is particularly suitable for (semi-)structural components utilising textile reinforcements (comprising of aligned, continuous yarns/tows that are knitted/woven/stitched/braided) in thermosetting matrices at high fibre fractions. Other than the potential to produce high-performance composites, LCM processes are specifically well suited to natural fibre reinforcements for a variety of reasons (Francucci et al. 2012a; Shah 2013b; Shah et al. 2013c):

1. Low processing temperatures (often <120 °C) during composite fabrication, thereby avoiding thermal degradation of natural fibres (which decompose above ~220 °C)
2. Minimal fibre damage during composite processing (as opposed to injection/extrusion moulding), thereby allowing retention of high reinforcement length, alignment and mechanical properties
3. Use of liquid resins with low viscosities (0.1–1 Pa s), thereby allowing good preform impregnation with low porosity even at low compaction/injection pressures
4. Use of thermosetting resins with polar functional groups that form a better interface with the (typically) polar surface of natural fibres (than polyolefin-based thermoplastics)
5. Relatively low-cost (and often unsophisticated) tooling, making the process compatible with low-cost plant fibres, particularly when manufacturing in less economically developed countries with an abundance of indigenous natural fibres
6. Closed-mould LCM processes reduce exposure to harmful emissions, therefore offering worker-friendly conditions, much like nonhazardous plant and animal fibres

Consequently, the LCM of NFRPs has received much recent attention in scientific research, where critical aspects such as reinforcement compaction (van Wyk 1946; Madsen 2004; Umer et al. 2011; Xue et al. 2011; Francucci et al. 2012a, 2013; Shah et al. 2014a) and permeability (Rodríguez et al. 2004; Francucci et al. 2010, 2013; Masoodi and Pillai 2011; Umer et al. 2011; Xue et al. 2011) and resin flow behaviour (Richardson and Zhang 2000; Rodríguez et al. 2007; Francucci et al. 2010; Masoodi and Pillai 2011; Xue et al. 2011) have been investigated. More recently, commercially viable, structural products have also been manufactured with NFRPs using LCM. These include the world's first flax composite 11 kW wind turbine blade developed by the University of Nottingham (Shah et al. 2013a) and Samsara's flax/hemp biocomposite surfboard (18/06/2012).

Here, we critically review the available literature on LCM of NFRPs. It is expected that the differences in structure (physical, chemical) of natural and synthetic fibres, their semi-products (i.e. yarns and rovings) and their textiles will have a perceptible effect on their processing via LCM. Consequently, we identify key findings concerning the reinforcement-related factors (namely, compaction and permeability) that influence, if not govern, the mould-filling stage during LCM of NFRPs.

## 4.2 Compaction Behaviour of Natural Fibre Reinforcements

### 4.2.1 Introduction

The first studies (Winson 1932; Schiefer 1933; van Wyk 1946) on fabric compaction were indeed based on natural fibres like wool, cotton and silk. The studies were, however, conducted by textile engineers to evaluate 'fabric handle', that is, the softness/smoothness, loftiness/resilience and drape of the material. Resistance to compression is still used as an effective parameter to measure the softness and pliability of garment textiles (Matsudaira and Qin 1995; Matsudaira 2006).

In contrast, in relation to composite manufacture, the compaction behaviour of technical textiles affects the reinforcement permeability and part fill time in the mould-filling process and also determines the thickness and volumetric composition (i.e. fibre volume fraction) of the final part (Long et al. 2005). Tight control of part thickness (and therefore weight) is a requisite for quality assurance in any composite manufacturing process. In addition, in their uncompressed state, textile reinforcements have a low fibre volume fraction [typically between 10 and 25 % (Long et al. 2005)]; for semi-structural applications this must be increased (to up to 70 %) during processing to exploit the mechanical properties of the reinforcement. Studying the relationship between compaction pressure  $P$  and fibre volume fraction  $v_f$  for a given preform also enables determining the maximum (practical) fibre volume fraction, which sets the upper limit of reinforcement efficiency. Consequently, compaction plays an important role in not only LCM processes but also in the stamping of textile-reinforced thermoplastic composites. Knowledge of the compaction behaviour of the reinforcement form is therefore critical.

While the compaction characteristics of synthetic reinforcements is well studied (Long et al. 2005), the compaction response of natural fibre reinforcements is a relatively new topic (van Wyk 1946; Madsen 2004; Umer et al. 2011; Xue et al. 2011; Francucci et al. 2012a, 2013; Shah et al. 2014a).

#### 4.2.1.1 Compaction Measurement and Modelling

Through-thickness compaction is usually measured by pressing flat preform layers between parallel metallic platens at a constant compaction speed (typically 0.5–5 mm/min) to a predetermined load (or pressure) or to a predetermined thickness (or fibre volume fraction) (Fig. 4.2). Tests can be conducted in dry (i.e. unsaturated) or wet (i.e. saturated in a test fluid) conditions. At the end of a compression cycle, the tester may (1) hold at constant load to measure creep, (2) hold at constant thickness to measure relaxation or (3) unload the sample (at the same rate) to measure hysteresis. Multiple repeat cycles can then be applied on the same specimen to examine the effects of rearrangement and compaction history.

From the compaction tests, plots of preform thickness  $t$  against compaction force  $F$  are obtained, which can be transformed into the more conventional plots of fibre volume fraction  $v_f$  against compaction pressure using Eq. (4.1) (Fig. 4.2).

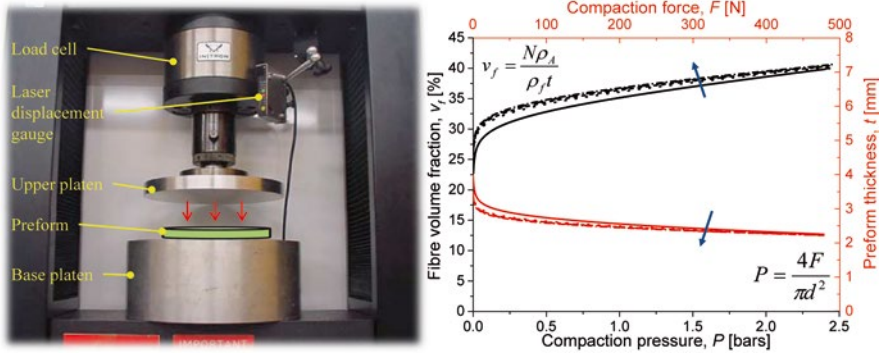


**Fig. 4.2** *Left*: testing rig for compaction of a dry reinforcement. *Right*: example compaction curves for a plain-woven flax fabric. The *arrows* indicate the direction in which the curves shift for the successive compaction cycles

$$v_f = \frac{N \rho_A}{\rho_f t}; \quad P = \frac{F}{A}, \quad (4.1)$$

where  $N$  is the number of layers,  $\rho_A$  is the areal density of a single layer,  $\rho_f$  is the fibre density and  $A$  is the sample press area.

At low compaction pressures ( $P < 0.1$  bar), the fibre volume fraction increases rapidly and the preform thickness decreases rapidly. Subsequent increase in compaction pressure pushes the fibre volume fraction and preform thickness to gradually approach an asymptotic maximum and minimum value, respectively. The experimental data is often approximated by models (assuming no rate dependence), where fitting parameters are representative of reinforcement properties (Robitaille and Gauvin 1998a, b; Correia et al. 2005; Long et al. 2005).

van Wyk (1946) and Gutowski et al. (1987a, b) independently proposed semi-analytical models for the compaction of random fibre mats (Eq. 4.2) and unidirectional plies (Eq. 4.3), respectively, assuming only fibre bending deformation. Both models incorporate fitting terms for the fibre volume fraction of the uncompacted preform  $v_0$  and the (bending) stiffness (spring constant)  $K$  of the reinforcement. Notably, van Wyk's work was based on the compaction of natural wool fibres, while Gutowski et al. (1987a, b) studied graphite fibres. For a variety of wool fibre mats, the reinforcement stiffness  $K$  in Eq. (4.2) was estimated to range from 10 to 40 MPa.

$$P = K v_0^3 \left( \frac{1}{v_f^3} - \frac{1}{v_0^3} \right), \quad (4.2)$$

$$P = K \frac{\left( \frac{v_f}{v_0} - 1 \right)}{\left( \frac{1}{v_f} - \frac{1}{v_{f,\max}} \right)^4}, \quad (4.3)$$

where  $v_{f,\max}$  is the maximum fibre volume fraction and  $K$  and  $v_0$  are empirical parameters representing reinforcement stiffness and uncompact fibre volume fraction, respectively.

More commonly, power-law regressions, of the form in Eqs. (4.4) and (4.5), are fitted to experimental compaction curves. Various researchers have employed Eqs. (4.4) (Madsen 2004; Xue et al. 2011) and (4.5) (Shah et al. 2014a) to accurately reproduce compaction data of various natural fibre reinforcements, obtaining non-linear least squares regression  $R^2$ -values  $>0.99$ .

$$v_f = a_1 \cdot P^{b_1}, \quad \text{where } P \text{ is in [Pa]}, \quad (4.4)$$

where  $a_1$  is the fibre volume fraction at 1 Pa and  $b_1$  is the stiffening index.  $a_1$  and  $b_1$  typically range between 0.02–0.12 and 0.1–0.2 for unidirectional plant fibre reinforcements and between 0.002–0.010 and 0.25–0.35 for random-mat plant fibre reinforcements (Madsen 2004).

$$v_f = v_0 + a_2 \cdot P^{b_2}, \quad \text{where } P \text{ is in [bar]}, \quad (4.5)$$

where  $v_0$  is the initial fibre volume fraction at no compaction pressure and  $a_2$  and  $b_2$  are the ‘additional’ fibre volume fraction (i.e.  $v_f - v_0$ ) at 1 bar and the reinforcement stiffening index, respectively.  $v_0$ ,  $a_2$  and  $b_2$  typically range between 0.3–0.4, 15–20 and 0.3–0.5 for woven silk textiles and between 0.2–0.3, 5–10 and 0.35–0.45 for woven plant fibre textiles (Shah et al. 2014a).

To compare materials that have been characterised with different models [e.g. Eqs. (4.4) and (4.5)], often the uncompact fibre volume fraction [indicated by  $a_1$  in Eq. (4.4) and  $v_0$  in Eq. (4.5)] and the fibre volume fraction at a reference compaction pressure are used.

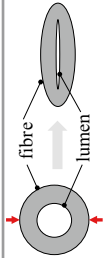
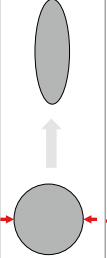
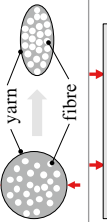
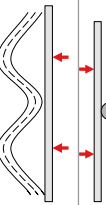
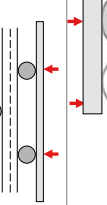
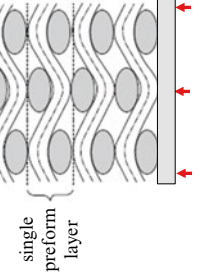
#### 4.2.1.2 Key Compaction Mechanisms

While empirical models are useful for inputs in process simulations, analytical studies provide an understanding of the mechanisms driving compaction (Chen and Chou 1999, 2000; Chen et al. 2001). Table 4.2 identifies the main factors contributing to the compaction of random-mat, nonwoven, and woven preforms. The primary and secondary mechanisms have been indicated. As shown in Fig. 4.3, natural fibre preforms experience all the compaction mechanisms that synthetic fibre preforms experience (Table 4.2), but not vice versa.

In particular, cross-section deformation at the fibre scale (Table 4.2) is limited to plant fibre reinforcements, which, due to their hollow nature and low transverse stiffness and strength (Shah et al. 2012a; Shah 2013b), undergo lumen closure and transverse cell-wall buckling and delamination during compaction (Lundquist et al. 2004; Francucci et al. 2012a, 2013). This is illustrated in Fig. 4.4. A substantial change in fibre cross-sectional shape is not unimportant in the context of preform compaction, as it may alter the potential for fibre relative motion and yarn



**Table 4.2** The dominant and secondary compaction mechanisms at the fibre, yarn and fabric scales in random-mat, nonwoven and woven preforms

Scale	Mechanism	Dominant in	Secondary in
Fibre/filament	 <p>Cell-wall/lumen collapse (fibre cross-section deformation)</p>	All plant fibre preforms	-
Yarn/tow	 <p>Yarn cross-section deformation</p>	All	-
Yarn/tow	 <p>Void condensation (i.e. closing gaps between fibres)</p>	Random mat	Woven and nonwoven
Yarn/tow	 <p>Yarn flattening</p>	Woven	Random mat
Yarn/tow	 <p>Fibre/yarn bending deformation</p>	-	All
Fabric/preform	 <p>Nesting and packing</p>	Woven	Nonwoven

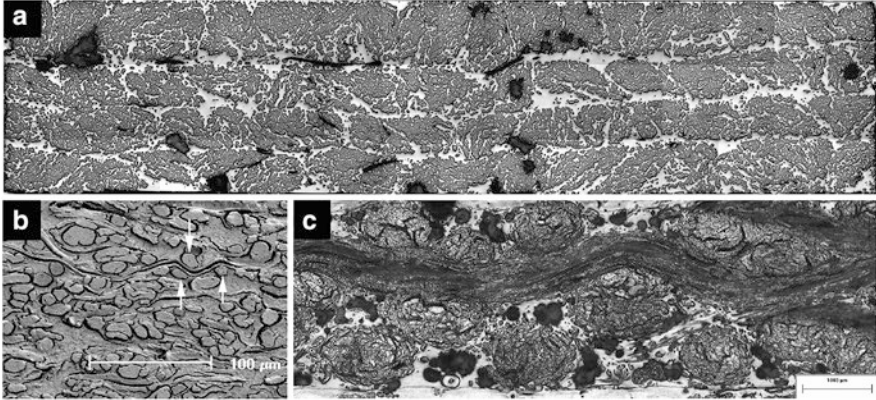


**Fig. 4.3** Compaction mechanisms in various natural fibre preforms: (a) yarn cross-section deformation, void consolidation and nesting/packing in a nonwoven unidirectional flax composite (Shah et al. 2011, 2014a, b; Shah 2013a, b). (b) Fibre bending and flattening and void consolidation in a random-mat wood fibre composite (Lundquist et al. 2004). Yarn cross-section deformation and flattening and nesting/packing in a woven flax composite (Goutianos et al. 2007)

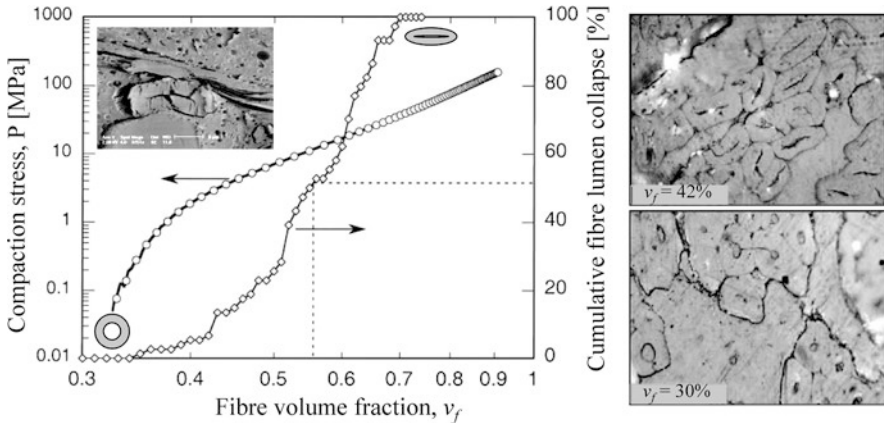


**Fig. 4.4** *Left*: increased compaction pressure on a wood pulp random mat increases the fibre volume fraction, with partial contribution from cumulative lumen collapse-associated fibre deformation (Lundquist et al. 2004). *Insert*: SEM depicts a collapsed fibre. *Right*: lumen collapse observed in a woven jute fabric due to increase in compaction pressure at higher fibre volume fractions (Francucci et al. 2012a)

reorganisation, and could possibly lead to hindered impregnation in localised interfibre zones.

Lundquist et al. (2004) found that lumen compression occurred between fibre volume fractions of 34 and 69 % in wood pulp random-mat preforms (Fig. 4.4). Void condensation is a dominant compaction mechanism, particularly at low compaction pressures (e.g. when  $v_f < 55$  %) in such random-mat preforms, with

fibre/yarn bending deformation and flattening being additional secondary mechanisms, particularly at high compaction pressures (e.g. when  $v_f > 55\%$ ). Francucci et al. (2012a) have also observed such irreversible transverse cell-wall deformation in compacted woven jute fabrics, and this phenomenon increased as the fibre content increased. They noted that this mechanism would contribute, alongside irreversible yarn cross-section deformation, yarn flattening and yarn nesting, to the compaction of the woven material. However, Francucci et al. opined that such lumen collapse would mostly occur when fibre rearrangement and tow movements are limited, i.e. at high fibre volume fractions. This is in stark contrast with the observation of Lundquist et al. (2004) described previously, where all wood pulp lumen had collapsed by  $v_f = 69\%$  and the wood pulp random mat was compressed further up to  $v_f = 90\%$ .

It is worth mentioning, however, that the luminal porosity in plant fibres varies between different species and even evolves with age within the same fibre. For instance, luminal porosities range between 74 and 80 % in kapok fibres, 20 and 70 % in wood fibres and 2 and 11 % in flax fibres (Shah 2013b). The luminal porosity has a significant effect on the transverse stiffness and yield strength in both compression and tension (Gassan et al. 2001; Lundquist et al. 2004; Placet et al. 2012), where fibres with a larger lumen (and smaller second moment of area) would tend to deform more readily. Naturally, therefore, different plant fibres would exhibit different degrees of fibre bending and cross-section deformation during plant fibre preform compaction.

Moreover, not all natural fibres have a central lumen; proteinaceous animal fibres like silk and wool are solid. Nonetheless, natural fibres tend to have low transverse properties due to their hierarchical, anisotropic structure (Ho et al. 2012; Shah et al. 2012a, 2014a). For instance, silks have a low transverse compressive modulus of 0.5–0.7 GPa (Ko et al. 2001) and a high Poisson's ratio of 0.4–0.5 (Zhang et al. 2010). Consequently, they undergo no change in cross-sectional area, but experience substantial deformation (i.e. flattening in cross-sectional shape) with increasing compressive force (Ko et al. 2001). While a 20 % reduction in thickness has been recorded for spider silk for compressive stresses of about 20 MPa (200 bar) (Ko et al. 2001), compaction pressures during LCM rarely exceed 1.5 MPa, below which the expected change in cross section is negligible.

Other micro- and macrostructural features, such as fibre cross-sectional shape and surface roughness (relating to fibre slippage) and degree of fibre alignment and dispersion, affect which (and when) compaction mechanisms will play primary and secondary roles.

#### **4.2.2 Through-Thickness Compaction of Natural Fibre Preforms**

The compaction response of reinforcement preforms is complex and depends on various elements, such as: type and form of fibre reinforcement, fibre architecture, number of layers in the preform, preform stacking sequence, history of loading, rate

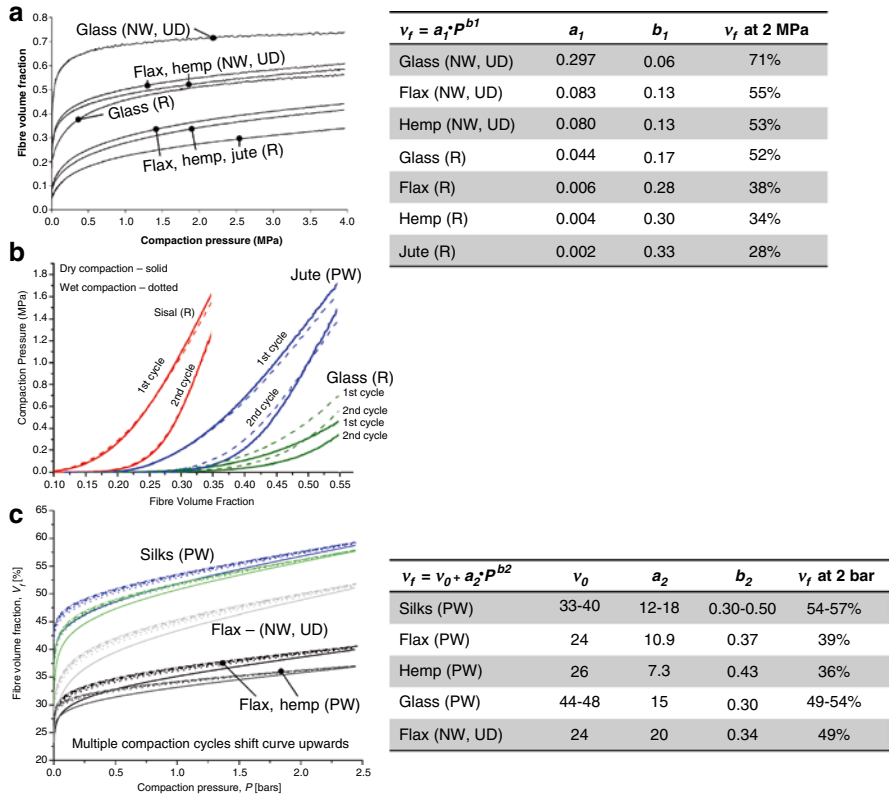


**Fig. 4.5** Compaction curves for various reinforcement preforms comparing the effect of fibre type and architecture. Plant fibre preforms are consistently less compactable than glass fibre preforms; natural silk preforms, however, are significantly more compressible than plant fibre preforms (and even more than glass fibre preforms—see text). Generally, nonwoven (NW) preforms tend to be more compactable than woven (W) preforms, which in turn are more compactable than random-mat (R) preforms. PW refers to plain-woven fabrics, while UD refers to unidirectional fabrics. The graphs are adapted from (a) Madsen (2004), (b) Francucci et al. (2013) and (c) Shah et al. (2014a). For reference, fitted model parameters are provided in the table

of compaction, tooling temperature and presence of lubricant (i.e. wet versus dry state) (Kim et al. 1991; Robitaille and Gauvin 1998a; Kelly et al. 2004; Correia et al. 2005; Long et al. 2005; Francucci et al. 2012a).

#### 4.2.2.1 Effect of Fibre Type on Single-Cycle Dry Compaction

The compaction behaviour of various reinforcement preforms is presented in Fig. 4.5. The data is a compilation from Madsen (2004), Francucci et al. (2013) and Shah et al. (2014a), where various natural fibre reinforcements have been characterised. Note that the preform architecture has a substantial effect on the compaction response of a material. In this section, we discuss the sole effect of the fibre type.

It is consistently observed that plant fibre reinforcements are considerably less compactable than synthetic fibre reinforcements, but natural silkworm silk fibres are as compactable as, if not more compactable than, glass fibres. It is notable that both the initial uncompactable fibre volume fraction [ $a_1$  in Eq. (4.4) and  $v_0$  in Eq. (4.5)] and the fibre volume fraction at a reference compaction pressure (e.g. 2 MPa or 2 bar) follow this trend (Fig. 4.5). This suggests that the compaction pressure needed to achieve any fibre volume fraction (within the range studied) is significantly lower in the case of silk and glass reinforcements than for plant fibre reinforcements. Moreover, amongst plant fibres, flax is found to be more compressible than hemp, which in turn is more compressible than jute.

Besides the differences in vertical positions (reflected by differences in fibre volume fractions at zero and reference compaction pressures), the shape of the compaction curves is also different for different fibre reinforcements. One could compare fitting parameters of Eqs. (4.4) (namely,  $b_1$ ) and (4.5) (namely,  $a_2$  and  $b_2$ ) to evaluate the differences in fibre type. For instance, glass and silk fibre reinforcements exhibit a steeper increase in fibre volume fraction at low compaction pressures than plant fibre reinforcements; this is indicated by small  $b_1$  values in Eq. (4.4) (Madsen 2004) and large  $a_2$  values in Eq. (4.5) (Shah et al. 2014a) (Fig. 4.5). For reference, fitted model parameters are presented in Fig. 4.5.

Analysing micro- to macrostructural features (i.e. fibre to yarn to fabric) in the silk, plant fibre and glass fibre reinforcements may explain these observations.

At the fibre scale, the (1) degree of fibre separation, (2) fibre surface roughness, (3) fibre cross-sectional shape and (4) fibre mechanical properties are notable factors. Firstly, preforms with well-separated fibres compact more readily due to increased degrees of freedom (Madsen 2004). While plant fibres typically exist as bundles, silk fibres, like synthetic glass fibres, are well separated from one another (Fig. 4.6a, b). Notably, it is the residue of the natural binding agent that dictates whether the fibres are separated or bundled. Pectin, the binding agent between elementary plant fibres to form a technical plant fibre bundle, is usually only partially decomposed during the fibre extraction process. On the other hand, the fibroin strand in silkworm silk is usually well degummed from the sericin binder. Secondly, the friction between fibre and fibre contacts is a relevant factor (Long et al. 2005), as fibre, yarns and fabric layers move (i.e. slide against each other) to dissipate energy during compaction. Plant fibres have a rougher surface than both silk and glass fibres (Fig. 4.6c, d), and consequently the latter may find it easier to adjust to a more efficient packing arrangement due to lower friction forces (Francucci et al. 2013; Shah et al. 2014a). Thirdly, the irregular almost-triangular cross-sectional shape of single silk fibres also permits higher ‘intra-yarn’ packing densities than irregular polygonal cross-sectional plant fibres (Fig. 4.6e, f) (Shah et al. 2014a). Finally, as the longitudinal and transverse elastic tensile moduli of a) silk and b) flax are a) 7–17 GPa and 0.5–0.7 GPa and b) 50–70 GPa and 4–9 GPa (Shah et al. 2012a), respectively, and as the ultimate failure strain of silk and flax is 15–30 % and 2–4 % (Shah et al. 2012a), respectively, silks can undergo much greater bending deformation without fibre breakage to enable efficient nesting and interlayer packing. In fact, fibre breakage and lumen collapse have been reported to be two critical mecha-

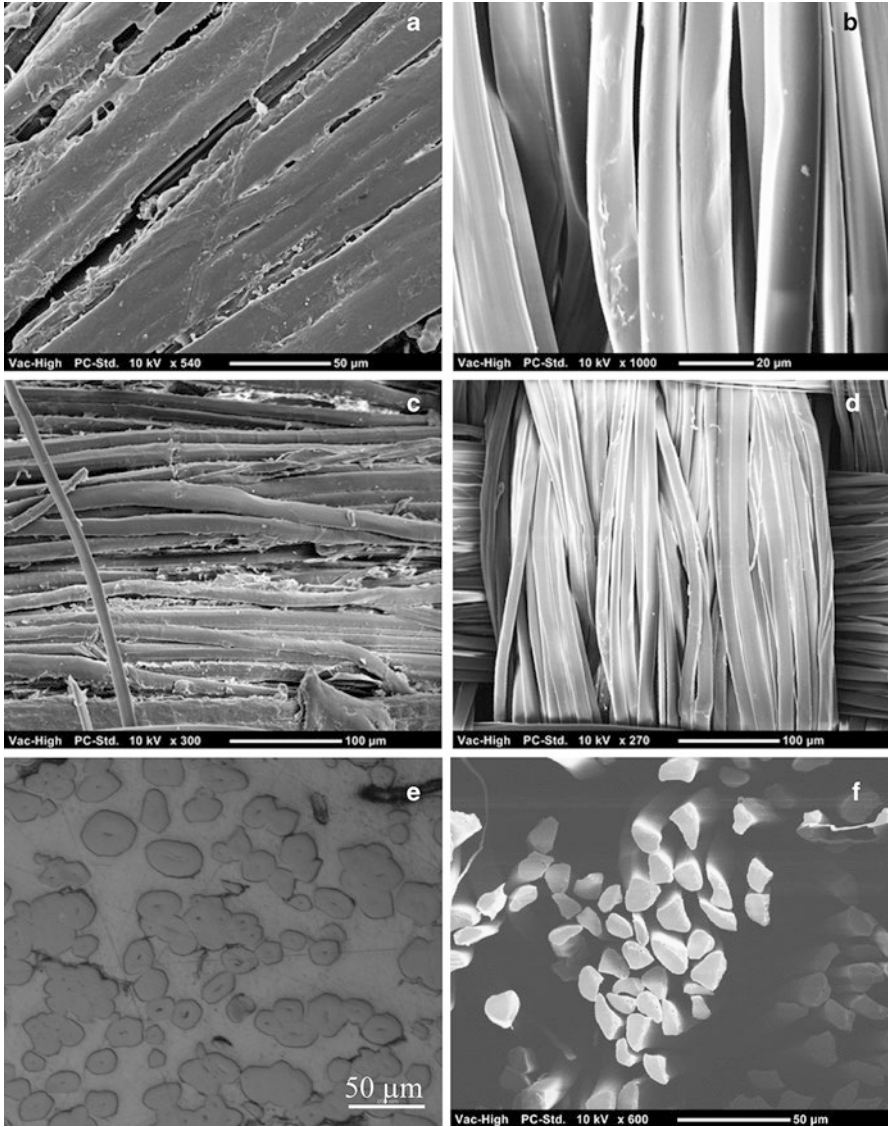


**Fig. 4.6** Micrographs depicting: (a) the bundled nature of plant fibres and (b) the fibrillated nature of silk fibres; (c) plant fibres have a rougher surface than (d) silk fibres; while (e) plant fibres have irregular polygonal cross-sectional shape, (f) silk fibres have irregular almost-triangular cross-sectional shape. From Shah et al. (2014a)

nisms responsible for the permanent deformation of plant fibre preforms during compaction (Francucci et al. 2012a). Glass fibres, on the other hand, are stiff, isotropic fibres. It would be expected that fibre bending would be a more dominant compaction mechanism in silk and plant fibre reinforcements than glass fibre reinforcements.

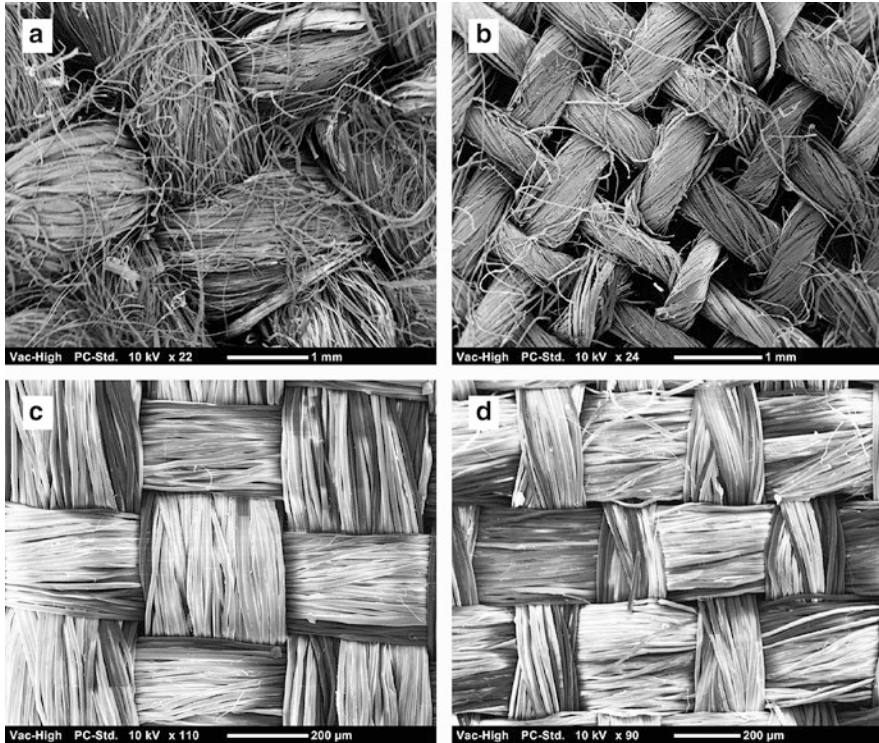


**Fig. 4.7** Micrographs depicting woven textiles of flax and hemp (a, b) and silk (c, d). From Shah et al. (2014a)

At the yarn and fabric scale, (1) yarn/fabric geometry and (2) fibre alignment are notable factors. Regarding fabric geometry, the tightness of a weave and inter-yarn porosity, for instance, will affect preform compactibility. Silk textiles, like glass fibre textiles, are more tightly woven than plant fibre textiles (Fig. 4.7), thereby imparting high packing density, particularly at low compaction forces. This would explain the high values of  $v_0$  and  $\alpha$  for silk textiles in comparison to plant fibre textiles (Shah et al. 2014a). Regarding yarn geometry, while plant fibre yarns tend to have a circular cross section due to high twist factors, silk fibre assemblies, much like glass fibre assemblies, have large width-to-thickness ratios (of  $\sim 5$ ). The lenticular cross-sectional shape of silk rovings would enable higher ‘inter-yarn’ compaction than twisted plant fibre yarns (Shah et al. 2014a). Moreover, this also reduces crimp. High crimp in woven fabrics would lead to higher ‘hills’ and lower ‘valleys’. It would be expected, therefore, that yarn bending deformation and nesting would be more important compaction mechanisms in plant fibre textiles than silk textiles.

Crimp is one source of fibre misorientation that has a detrimental effect on compaction. In terms of orientation, the arrangement of yarns in the fabrics is clearly more ordered and uniform in the silk textiles (Fig. 4.7). Studies on the compaction of both E-glass and plant fibre reinforcements have reported that rovings are

significantly more compactable than twisted yarns (Kim et al. 1991; Madsen 2004). This is because yarn twist induces fibre misorientation and transverse pressure, both of which are detrimental to effective packing (Shah et al. 2013b). Note that twist is a 3D phenomenon and that yarn twist (and yarn packing fraction) are a function of yarn radius; the twist angle and packing fraction are highest and lowest, respectively, at the yarn surface (Shah et al. 2013b). As observed in Fig. 4.7, while the plant fibre textiles employ yarns that are twisted (surface twist angle of 20–30°), the silk textiles employ rovings of well-aligned filaments.

Studies have shown that not only yarn twist but yarn hairiness (or fluffiness) is also an important source of misorientation (Kim et al. 1991). Elementary plant fibres have non-uniform width in the range of 10–100  $\mu\text{m}$  and a short length in the range of 4–100 mm (Lewin 2007). Due to the short length of staple plant fibres, during the spinning process not all fibre ends are integrated into the yarn structure. The distribution (length and frequency) of fibre ends protruding from the fibre surface is referred to as yarn ‘hairiness’ by textile engineers. These protruding fibres have a negative impact on the packing of a fabric preform. Kim et al. (1991) report that the compaction response of a fluffy roving may be as poor as that of a twisted spun yarn, relative to a straight roving; for instance, straight roving preforms have fibre volume fractions of 70 % at compaction pressures of 2 MPa, compared to fibre volume fractions of only 50 % for both fluffy roving and spun yarn preforms. As observed in Fig. 4.7, numerous fibres are protruding from the structure of the yarns in the flax textiles, while filaments in the silk fibre textiles are well integrated into the roving. It is noteworthy that the sources of misorientation (yarn twist and yarn hairiness) are lacking in silk textiles because silks exist as long fibres (i.e. filaments), unlike staple plant fibres. In fact, silks, such as those industrially processed from the silkworm cocoons, exist as single continuous filaments/strands of fibroin with lengths of up to 1,500 m (Lewin 2007). Put it simply, it is easier to align longer fibres than shorter fibres.

#### 4.2.2.2 Effect of Fabric Architecture

As shown in Table 4.2, the fabric architecture plays a key role in determining the mechanisms that drive compaction. The effect of fabric architecture on the compaction of synthetic fibres has been studied in some detail (Kim et al. 1991; Robitaille and Gauvin 1998a; Yang et al. 2012) and similar trends have been reported in the limited articles investigating natural fibre reinforcements (Madsen 2004; Francucci et al. 2013; Shah et al. 2014a).

As observed in Fig. 4.5, unidirectional nonwovens tend to be more compactable than woven fabrics, which in turn are more compactable than random-mat reinforcements. Notably, the compaction curves shift upwards [i.e. higher fibre fractions at zero [ $a_1$  in Eq. (4.4) and  $v_0$  in Eq. (4.5)] and reference compaction pressures], exhibit a steeper rise at low compaction pressures [i.e. smaller  $b_1$  in Eq. (4.4) and larger  $a_2$  in Eq. (4.5)] and become more flat at high compaction pressures.



Fibre alignment/orientation is a mechanism-governing factor in fabric architecture. For instance, in unidirectional fabrics, fibres in adjacent layers are parallel to each other and can therefore fill gaps by dislodging other fibres to produce a compact structure. In woven fabrics, however, fibres/yarns leave voids during crossover (weave density) that cannot be filled by crossover fibres in other layers. Essentially, fibre packing between layers with the same fibre/yarn orientation is easier than packing between layers with different fibre/yarn orientations. Of course, in aligned reinforcements (nonwoven and woven), the stacking sequence also affects the compaction response, but this has not been studied on natural fibre reinforcements so far.

Alongside fibre orientation, fibre/yarn length and diameter may also affect pre-form compaction. Umer et al. (2011) and Madsen (2004) investigated the compaction behaviour of random mats constructed with yarns of varying length and diameter. Madsen (2004) found that compaction curves of hemp yarn random mats, with mean yarn lengths of 2, 10 and 50 mm, were nearly identical. In contrast, Umer et al. (2011) observed that the required compaction pressure for 50 mm flax yarn random mat was about 40 % higher in comparison to a 15 mm flax yarn random mat. They attributed the poorer compactibility of longer yarn mats to the larger number of bundle–bundle crossover points. Umer et al. (2011) also found that flax random mats were significantly more compactable when larger diameter yarns were employed. They suggested that there were more fibres in larger diameter yarns that were more efficiently packed within the available space (than they would be as loose fibres in the mat), and consequently there were less fibre crossover points within the mat.

#### 4.2.2.3 Effect of Multiple Compaction Cycles

Multiple compaction cycles have a noticeable and well-documented effect on pre-form compaction (Kim et al. 1991; Robitaille and Gauvin 1998a; Long et al. 2005). Natural fibre reinforcements, like synthetic fibre reinforcements, follow the general trend (Madsen 2004; Francucci et al. 2012a; Shah et al. 2014a): (1) in comparison to the first cycle, the second compaction cycle requires a relatively lower compaction pressure to achieve a given fibre volume fraction, (2) subsequent compaction cycles (i.e. third, fourth and fifth) overlay with the second compaction cycle, and (3) all compaction curves share the same asymptotic fibre volume fraction (at very high compaction pressures) (Fig. 4.5). With regard to the fitting model parameters, in comparison to the first compaction cycle, the uncompressed fibre volume fraction [ $a_1$  in Eq. (4.4) and  $v_0$  in Eq. (4.5)] tends to increase and a steeper rise at low compaction pressures is observed [i.e. smaller  $b_1$  in Eq. (4.4) and larger  $a_2$  in Eq. (4.5)] for the second compaction cycle. Subsequent compaction cycles have fairly identical fitting parameters to the second cycle.

Maximising the fibre content is appealing for NFRPs, not only to improve composite mechanical performance (Shah et al. 2012b; Shah 2013b) but also to increase the content of bio-based material and reduce the amount of polymer.

The latter improves sustainability credentials as natural fibres require significantly less energy for production than both synthetic fibres and polymer matrices (Duflou et al. 2012; Shah 2013b). The aforementioned findings provide useful insights in developing high fibre content NFRPs. If high compaction pressures, such as those realised using an autoclave for LCM (up to 15 bar) or a mechanical press for compression moulding (up to 100 bar), are used, a single compaction cycle is sufficient. That is, pre-compaction is not necessary. However, if low compaction processes are employed, such as in vacuum bagging, pre-compaction of the reinforcement is an attractive technique to improve preform compaction and increase the part fibre volume fraction.

Notably, multiple compaction cycles generally lead to the reorganisation and permanent deformation of fibres/yarns within the textiles, driven through both elastic and irreversible mechanisms, such as those illustrated in Table 4.2. Compaction mechanisms such as fibre/yarn cross-section deformation, yarn flattening and nesting tend to become more significant at higher compaction pressures (and thus fibre volume fractions) (Francucci et al. 2012a); therefore, the maximum compaction pressure of the previous cycle has an effect on the compaction in the next cycle. In addition, stacked textiles have a time-dependent viscoelastic behaviour (Francucci et al. 2012a); therefore, studying preform relaxation is as important as studying preform compaction. In fact, relaxation studies post-multiple compaction cycles have revealed that plant fibre reinforcements undergo significantly more irreversible, permanent deformation than glass fibre reinforcements (Francucci et al. 2013).

#### 4.2.2.4 Wet Compaction

In LCM, while the preform is first compacted in the dry state (in the mould-filling stage), once the preform has been impregnated, the saturated preform undergoes 'wet compaction' (in the post-filling stage) (Table 4.1). During and post-impregnation, the compaction pressure exerted on the partially or fully saturated preform is only partially felt by the reinforcement; the remaining compaction pressure is managed by the liquid resin (Long et al. 2005). However, lubricating effects of the liquid tend to reduce the compaction pressure required to achieve a given fibre volume fraction. This is because lubrication of fibre-to-fibre contact points means that individual fibres find it easier to move and slide and realign and reorganise. As a corollary, it is also expected that as the fibres are likely to attain a higher degree of stability for a given compaction pressure, the preform would exhibit less relaxation (when held at a constant thickness). These assertions have been found to be true for synthetic fibre preforms (Kim et al. 1991; Long et al. 2005).

Natural fibres, including plant and animal fibres, are different from synthetic fibres like glass, in that natural fibres tend to be polar and hydrophilic. That is, natural fibres absorb polar liquids; this not only includes liquids used during compaction and permeability testing like water and glycerine solution but also includes polar thermosetting resins such as vinyl ester and phenolics (Francucci et al. 2010). Moreover, natural fibres swell upon liquid absorption (10–25 % moisture regain) (Francucci et al. 2010).

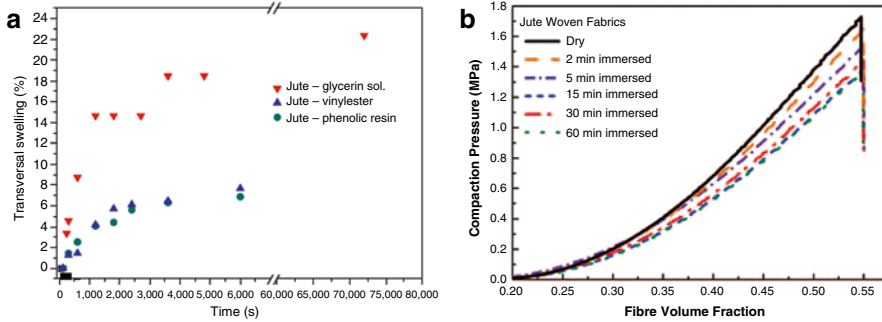


**Fig. 4.8** (a) Transverse swelling (in terms of % diameter change) of jute fibres in different fluids. Adapted from Francucci et al. (2010). (b) Effect of immersion time on the compaction of jute woven fabrics. From Francucci et al. (2013)

For instance, over an immersion time of 6,000 s, jute fibres exhibited equilibrium transverse swelling (i.e. change in diameter) by over 18 % in glycerine solution and between 6 and 8 % in vinyl ester and phenolic resin (Fig. 4.8a). In comparison, glass fibres do not absorb liquid (<2 % moisture regain), nor do they exhibit swelling (Francucci et al. 2010).

As natural fibres absorb liquids and consequently swell and soften (Francucci et al. 2010, 2013), their wet compaction behaviour requires attention. Since natural fibres will behave differently with different liquids (say, nonpolar oils as test fluids and polar epoxy resin as the matrix), to understand their true compaction behaviour, the natural fibre reinforcement should be studied with the particular resin that is to be used during LCM as the test fluid.

Investigations on plant fibre reinforcements have found that the immersion time is an important test parameter (Francucci et al. 2013). In comparison to the compaction curve of a dry reinforcement, the compaction curve of plant fibre reinforcements shifts to higher fibre volume fractions (i.e. enhanced compactibility) with increasing immersion time of the saturated preform (Fig. 4.8b). This is similar to synthetic fibre performs. However, it is found that the wet relaxation behaviour of plant and synthetic fibre reinforcements stands in contrast, with plant fibre reinforcements showing greater relaxation in the wet state in comparison to the dry state (rather than the expected less relaxation). Francucci et al. (2013) propose that the observed result is due to fibre softening upon swelling during wet compaction.

#### 4.2.2.5 Effects of Other Parameters

The effects of other parameters, such as number of layers and compaction rate, on the compaction behaviour of natural fibre reinforcements have been studied in literature (Francucci et al. 2012a, 2013; Shah et al. 2014a). Generally, their effects are relatively weak, and notably conflicting trends have been reported for synthetic fibre reinforcements.

Shah et al. (2014a) observed that reducing the number of layers of woven silk fabric shifted the compaction curves marginally to higher fibre volume fractions (i.e. enhanced compactibility). Moreover, the curves became steeper at higher compaction pressures. These are indicative of the fact that stacks made of less fabric layers are easier to compact to a given fibre volume fraction, particularly at higher compaction pressures, because nesting, the primary compaction mechanism of woven textiles, becomes progressively difficult with more layers (Long et al. 2005), potentially due to the non-uniform transmission of the applied compressive force through the textile layers.

Conflicting, though weak, trends have been observed on the effect of compaction speed on natural fibre reinforcement compaction. Shah et al. (2014a) reported that woven silk textiles were more compactable at higher compaction rates. For instance, a 100-fold increase in the compaction speed from 0.5 to 50 mm/min increased  $v_0$  from 30.5 to 32.2 % and increased the representative fibre volume fraction  $v_f$  at  $P=2.0$  bar from 53.7 to 54.1 %. In comparison, Francucci et al. (2012a) found that increasing the compaction speed led to a larger compaction pressure for the same fibre volume fraction of woven jute fabrics.

### 4.2.3 Conclusions

The compaction response of natural fibre reinforcements can be characterised by the same power-law regression curves as synthetic fibre reinforcements. Good reproducibility of test measurements and strong model curve fits are found. Natural fibre reinforcements also show evidence of similar compaction mechanisms as synthetic fibre reinforcements, with the addition of fibre cross-section deformation through cell-wall and lumen collapse in the case of hollow plant fibres.

In general, plant fibre reinforcements are significantly less compactable than glass fibre reinforcements. However, animal silk fibre reinforcements demonstrate comparable compactibility to the latter. The difference in structure (i.e. geometry, alignment and dispersion) and technical properties of the fibres, their semi-products (i.e. yarns and rovings) and their textiles accounted for the differences in fabric compaction behaviour. Unlike plant fibres, silk, the only natural fibre to exist as long filaments (rather than short fibres), and its semi-products and textiles have much resemblance with synthetic fibres and their semi-products and textiles.

The effects of fabric architecture, multiple compaction cycles, compaction rate and number of layers of fabric on preform compaction follow the same generic trends in natural and synthetic fibre reinforcements. However, irreversible, permanent deformation during compaction is more prevalent in plant fibre reinforcements than glass fibre reinforcements. More studies on the creep and relaxation response of natural fibre reinforcements are therefore required. For low-pressure LCM processes (such as vacuum bagging), pre-compaction through an initial single cycle is identified to be an attractive technique to improve compaction and part fibre volume fraction.

The wet compaction of natural fibre reinforcements requires specific attention, as unlike synthetic fibres, natural fibres absorb the liquid resin and swell and soften. This not only affects the relaxation response of the saturated reinforcement but also its permeability. Moreover, as natural fibres will behave differently with different fluids, the fibre compaction behaviour needs to be studied for the specific resin that is to be used during composite manufacture.

### **4.3 Modelling the Mould-Filling Process in LCM of Natural Fibre Composites**

Controlled and complete filling of the mould with adequate wetting of fibres is a primary objective in LCM. Poor fibre wetting would lead to poor mechanical properties due to micro-void formation and poor interfacial adhesion, while uncontrolled and incomplete filling would lead to defect formation (e.g. dry spots), poor part quality and even part scrappage and material wastage. Optimising mould fill time while avoiding fluid pressure build-up is another important aspect of controlled mould filling. The microscopic and macroscopic flow of the liquid resin through gaps within yarns/tows and the porous preform, respectively, is therefore important to study.

A number of factors affect the complex mould-filling process (Table 4.1), including preform permeability, inlet/outlet gate location, pressure differential in mould cavity, rate of resin injection and resin viscosity (as a function of time). Extensive research has been conducted to measure, predict and simulate the mould-filling process in the LCM of conventional synthetic fibre composites (Long et al. 2005). Often, permeability studies and Darcy's law [which can be derived from the Navier–Stokes equation through averaging methods (Neuman 1977)] are used to model the complicated viscous flow of resin in a porous media. Natural fibre reinforcements, however, require specific considerations.

#### ***4.3.1 In-Plane Permeability of Natural Fibre Reinforcements***

Permeability is defined as the ease of fluid flow through a preform, and therefore it is an inverse measure of the flow resistance (Long et al. 2005). The greater the preform permeability, the easier it is for the resin to impregnate the reinforcement, and the lesser the time needed to fill the mould. Fabric permeability has a governing effect not only on fill time and flow front shape but also on void and dry-spot formation resulting from the dual-scale flow within preforms (Fig. 4.9) and the anisotropic permeability of anisotropic preforms.

While permeability characterisation of natural fibre reinforcements is a relatively new topic (Rodriguez et al. 2004; Francucci et al. 2010, 2013; Masoodi and Pillai 2011; Umer et al. 2011; Xue et al. 2011), researchers have already found some critical differences between natural and synthetic fibre reinforcements. These will be discussed in this section.

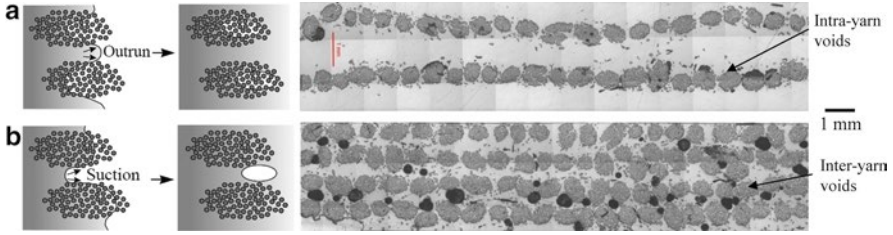


**Fig. 4.9** The complex, dual-scale flow of resin in fibrous preforms can generate voids. Macroscale flow relates to the advance of resin between yarns/tows (i.e. inter-yarn flow), while microscale flow relates to the penetration of resin into a yarn (i.e. intra-yarn flow). Note that permeability is also different at the two scales. For instance, (a) at low fibre content, due to low yarn permeability but high overall permeability, the yarn is not properly impregnated and thus intra-yarn voids may form, while (b) at high fibre content, although yarn and overall permeability are similar, capillary flow in the yarn dominates and therefore inter-yarn voids are formed. From Shah et al. (2012b) and Shah (2013a)

#### 4.3.1.1 Permeability Measurement and Modelling

Typically, preform permeability is experimentally measured by tracking the progression of the fluid flow front and monitoring the pressure field (Fig. 4.10). A planar flow cell is used in which a test fluid (with a similar viscosity as the resin) is injected into the fabric. A 1D unidirectional flow achieved through line-gate injection (Fig. 4.10a, b) is commonly used. However, a 2D radial flow achieved through central injection (Fig. 4.10c, d) may be more appropriate for anisotropic reinforcements to quickly measure anisotropy in permeability. The fluid viscosity is measured using a viscosimeter or rheometer. A flowmeter, typically placed at the inlet or outlet port, may be used to measure fluid velocity. Alternatively, the flow velocity may be estimated by measuring flow front evolution. The flow front can be tracked manually (e.g. with scale bars, as in Fig. 4.10b), with a video camera, or even electrically activated (pressure) sensors. Pressure gradient in the mould may be recorded through manometers or pressure transducers, typically placed at the inlet and outlet ports. Pressure difference is measured relative to the flow front (which is at atmospheric pressure).

Darcy's law, which describes the flow of Newtonian fluids in porous media, is then used to determine permeability. Assuming steady-state 1D flow, Darcy's law (Eq. 4.6) states that the macroscopic volumetric flow rate  $Q$  is proportional to the mould cross-sectional area  $A$  and the pressure difference over the sample  $\Delta P$  and inversely proportional to the sample length  $L$  (in the flow direction) and fluid viscosity  $\mu$ . The constant  $K$  is termed the permeability.

$$Q = K \frac{A \Delta P}{L \mu}. \quad (4.6)$$

Saturated (or steady-state) permeability  $K_{\text{sat}}$  is obtained once the reinforcement is fully saturated, using Eq. (4.7). On the other hand, unsaturated (or transient)

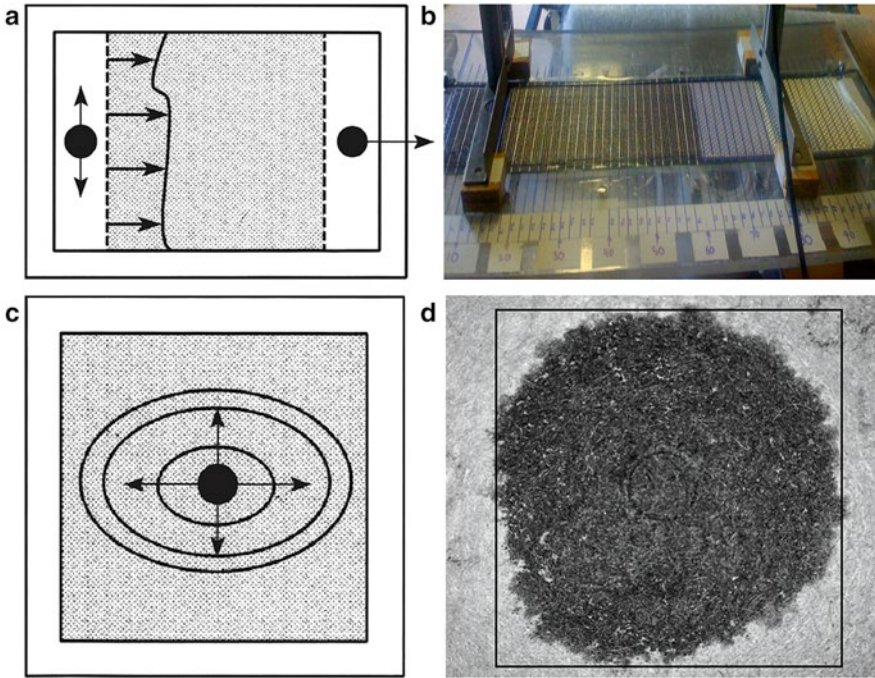


**Fig. 4.10** Permeability measurement and flow visualisation set-ups. (a, b) 1D linear flow through line-gate injection (Parnas et al. 1995). (c, d) 2D radial flow through central injection (Parnas et al. 1995; Xue et al. 2011)

permeability  $K_{\text{unsat}}$  is obtained when the flow profile is measured during the injection process. Darcy's law in Eq. (4.6) can be integrated and rearranged to the form in Eq. (4.8) (Cai 1992), where  $x$  is the position of the flow front at time  $t$ ,  $\phi$  is the fabric porosity, and  $v$  is the average fluid velocity. Note that fabric porosity is directly related to the fibre volume fraction. For demonstration, Fig. 4.11a shows the linear relationship between the square of the flow front position and fill time, for two separate infusion conditions; the slope of the curve  $x^2/t$  is used as an input in Eq. (4.8) to determine  $K_{\text{unsat}}$ .

$$K_{\text{sat}} = Q \frac{\mu}{\Delta P} \frac{L}{A}, \quad (4.7)$$

$$K_{\text{unsat}} = \frac{x^2}{t} \frac{\phi \mu}{2 \Delta P}, \quad \text{where } \phi = \frac{Q}{vA} \quad \text{and} \quad \phi \equiv 1 - v_f. \quad (4.8)$$

The saturated and unsaturated permeability can be then determined over various conditions, say varying fabric porosity (or fibre volume fraction) as shown in Fig. 4.11b. In fact, reinforcement fibre volume fraction, alongside reinforcement type and orientation, is a key reinforcement-related factor affecting permeability.

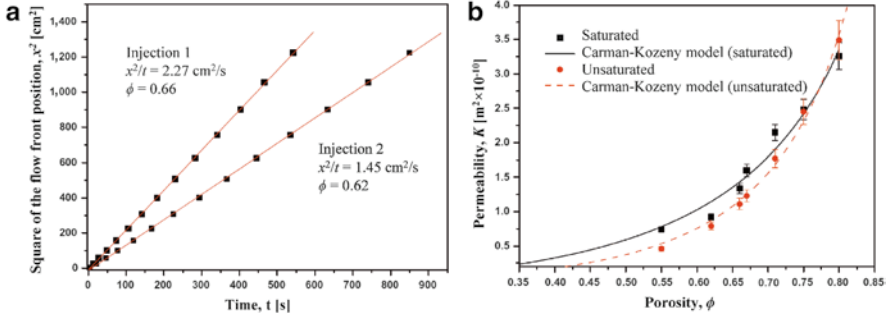


**Fig. 4.11** Permeability testing of woven jute fabric (Francucci et al. 2010). (a) Plot of square of flow front position with time for different infusion conditions. (b) Plot of saturated and unsaturated permeability against porosity (=1—fibre volume fraction)

Increasing the fibre content (decreasing porosity) reduces the number of flow paths and therefore reduces permeability. Often, the three-parameter exponential function [Eq. (4.9); proposed by Gauvin et al. (1994)] or the two-parameter, modified Carman–Kozeny equation (Carman 1937) (Eq. 4.10) is used to model permeability–porosity relationship. Both models are found to be well suited to natural fibre reinforcements (Rodriguez et al. 2004; Francucci et al. 2013).

$$K = a + b \cdot \exp^{c\phi}, \quad (4.9)$$

$$K = \frac{\phi^{n+1}}{C(1-\phi)^n} = \frac{(1-v_f)^{n+1}}{Cv_f^n}. \quad (4.10)$$

Two problems commonly associated with permeability testing are mould deflection (induced by the pressure gradient on thin moulds) and uncontrolled flow (Parnas et al. 1995). The latter may manifest in the form of fibre washing or edge effects. Fibre washing refers to the displacement of the preform during filling, while edge effects, also known as race-tracking, refer to the faster flow of resin at the edges due to lower permeability resulting from a clearance between the fibre preform and the mould edge. Indeed, such concerns have been voiced in studies on the mould-filling process of natural fibre reinforcements as well (Fig. 4.12) (Richardson and Zhang 2000; Rodriguez et al. 2004; Francucci et al. 2010; Ho et al. 2012). Fibre washing is more prevalent at high injection pressures and low fibre volume fractions (e.g. fewer reinforcement layers), while edge effects are more prevalent at high fibre volume fractions (Richardson and Zhang 2000).

#### 4.3.1.2 Effect of Reinforcement Type

The limited research on permeability studies of natural fibre reinforcements shows that while plant fibre reinforcements exhibit higher permeability than glass fibre reinforcements (Fig. 4.13) (Rodriguez et al. 2004; Francucci et al. 2013), wood fibre



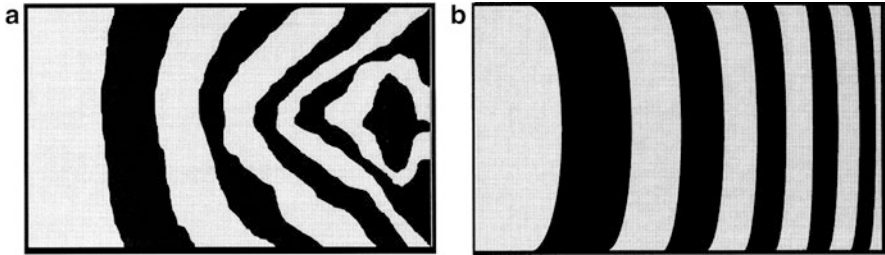


**Fig. 4.12** Resin flow in 2-layer random-mat hemp reinforcements before (a) and after (b) problems of fibre washing and edge flow were resolved. The flow front is smoother, more uniform and quasi-1D in (b). Flow front isochrones are shown, where each isochrone represents 20 s. Mould-filling direction is from *left to right*. From Richardson and Zhang (2000)

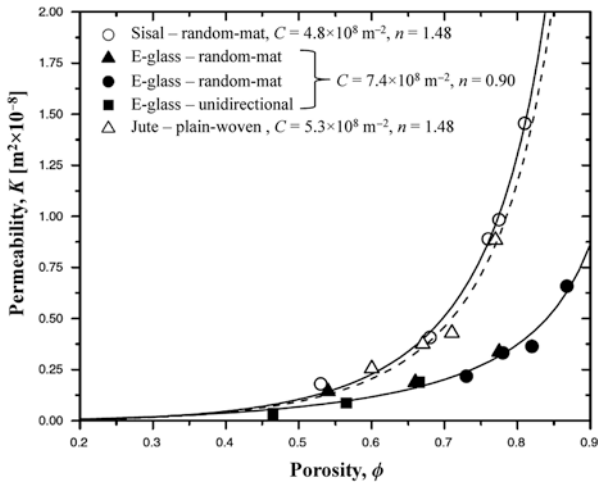


**Fig. 4.13** Comparison of the (unsaturated) permeability of sisal, jute and E-glass reinforcements. Carman–Kozeny constants are also provided. Adapted from Rodriguez et al. (2004)

mats exhibit significantly lower (by about two orders of magnitude) permeability than glass fibre mats (Umer et al. 2008). Table 4.3 describes permeability data of various natural fibre reinforcements studied in literature, by showing Carman–Kozeny constants and permeability values at specific fibre volume fractions. Notably,  $n$  is close to 2 in most cases, implying that the fluid flow behaviour in natural fibre reinforcements is close to the original Carman–Kozeny model, where fibre arrangement can be described as parallel tubes with low tortuosity (Rodriguez et al. 2004).

Researchers have hypothesised that the higher flexibility of plant fibres in comparison to glass fibres may make the former more permeable (Rodriguez et al. 2004). On the other hand, the lower permeability of wood fibre mats (in comparison to glass fibre mats) has been attributed to the more tortuous flow paths in the less-efficiently packed wood fibre mats, owing to the very short length of wood fibres (Masoodi and Pillai 2011). The argument may have merit as flax yarn random mats composing of

**Table 4.3** Permeability data of various natural fibre reinforcements

Reinforcement	$C$ [ $\times 10^8 \text{ m}^{-2}$ ]	$n$	$K$ at $v_f = 0.2$ (or $\varphi = 0.8$ ) [ $\times 10^8 \text{ m}^{-2}$ ]	$K$ at $v_f = 0.5$ (or $\varphi = 0.5$ ) [ $\times 10^8 \text{ m}^{-2}$ ]	Unsaturated or saturated, test fluid, viscosity	Source
Wood fibre – random-mat	2460	1.80	0.00394	0.000203	Saturated Mineral oil, 0.066-0.095 Pa·s	(Umer 2008)
Wood fibre – random-mat	4000	1.76	0.00229	0.000125	Saturated Mineral oil, 0.066-0.095 Pa·s	(Umer 2008)
Sisal – random-mat	4.8	1.48	1.30	0.104	Unsaturated, Glycerine solution, 1.2 Pa·s	(Rodriguez 2004)
Jute – plain-woven	5.3	1.48	1.17	0.0943	Unsaturated, Glycerine solution, 1.2 Pa·s	(Rodriguez 2004)
Sisal – plain-woven	22.5	2.00	0.569	0.0222	Unsaturated, Vinylester resin, 0.5-0.9 Pa·s	(Li 2006)
Jute – plain-woven	81.0	0.88	0.0335	0.00617	Saturated, Glycerine solution, 0.13 Pa·s	(Francucci 2013)
Jute – plain woven	133.8	1.29	0.0357	0.00373	Unsaturated, Glycerine solution, 0.15 Pa·s	(Francucci 2010)
Jute – plain woven	84.6	0.91	0.0334	0.00591	Saturated, Glycerine solution, 0.15 Pa·s	(Francucci 2010)

longer fibres have notably and consistently higher (saturated) permeability across a range of fibre volume fractions (Umer et al. 2011). For instance, the permeability of random mats with 50 mm fibre lengths was found to be 22 and 25 % higher at the lowest ( $v_f=0.2$ ) and highest ( $v_f=0.4$ ) fibre volume fractions, in comparison to random mats with 15 mm fibre lengths (Umer et al. 2011).

Yarn diameter (or linear density) is also known to affect the permeability of flax yarn random mats (Umer et al. 2011). Umer et al. (2011) found that the permeability of medium yarn diameter (0.56 mm) mats was consistently (i.e. over a range of porosity levels) 27 % higher than small yarn diameter (0.35 mm) mats, but the permeability of small and medium yarn diameter mats was consistently 68–77 % higher than large yarn diameter (0.81 mm) mats. Given that the permeability of preforms is dominated by the characteristics of open channels and that preform geometric parameters that describe the characteristics of the open channels include the number of fibres in the bundle, twist angle and orientation of bundle, dimension and cross-sectional shape of bundles and single fibres, Umer et al. suggested that large diameter yarns were less compact and had lower twist levels. The loose fibres on the surface (previously referred to as hairiness) of large diameter yarns restrict fluid flow through the open channels, thereby decreasing permeability. The twist level of yarns may also affect permeability and impregnability by altering competition

between micro-flow and macro-flow (Goutianos and Peijs 2003; Umer et al. 2011; Shah 2013a); this is discussed further in Sect. 4.3.1.5.

It is clear from Table 4.3 that experimental conditions have a notable effect on the permeability data obtained for even the same natural fibre reinforcement (e.g. jute plain-woven fabric). In particular, it is important to clarify (1) whether it is the saturated or unsaturated permeability that has been measured, (2) the test fluid viscosity and (3) the polarity of the test fluid. While the first two issues apply to reinforcement preforms in general, the latter point applies specifically to natural fibre reinforcements. For natural preforms, saturated permeability tends to be higher than unsaturated permeability (Francucci et al. 2010) [discussed in Sect. 4.3.1.4], and permeability tends to be lower when measured in less viscous fluids (which is also in agreement with Eqs. (4.7) and (4.8)). The more interesting issue is of the polarity of the test fluid, as natural fibres, unlike synthetic fibres, absorb polar fluids and consequently swell and soften (Umer et al. 2007; Francucci et al. 2010). This was discussed previously in Sect. 4.2.2.4. Conceivably, fluid absorption and swelling are important mechanisms in natural fibre preforms, due to which both saturated and unsaturated permeability are reduced. Francucci et al. (2010) demonstrated through absorption, swelling and permeability tests on untreated and treated jute fibre random mats that untreated mats had up to five times higher absorption levels, up to 20 times higher transverse swelling and an order of magnitude lower permeability than treated mats. Umer et al. (2007) show that permeability levels of wood fibre mats measured in (polar) glucose syrup were lower than that measured in (nonpolar) mineral oil. Fluid absorption removes fluid from the main stream, acting as a sink component and thus decreasing flow velocity during the unsaturated flow. The swelling of the natural fibres constricts the open flow path, reduces porosity and increases flow resistance during saturated flow. Since natural fibres will behave differently with different liquids, to accurately measure their permeability, the natural fibre reinforcement should be studied with the particular resin that is to be used during LCM as the test fluid.

#### 4.3.1.3 Permeability Anisotropy

Random mats are quasi-isotropic reinforcements and would therefore produce quasi-isotropic flow due to quasi-isotropic permeability. Xue et al. (2011) measured the anisotropy ratio in permeability ( $K_{\max}/K_{\min}$ ) to range between 1.08 and 1.46 for flax random mats; cross-laid mats were more isotropic than parallel-laid mats. Orientation distribution analysis showed that fibres were uniformly distributed in cross-laid mats, but fibres in parallel-laid mats were oriented primarily along the machine direction. As the preferential resin flow path (path of least resistance) would be along the principal fibre orientation direction, permeability was much higher in this direction, for parallel-laid mats. In cross-laid mats, due to fairly equal paths of least resistance, flow was more isotropic. Note that interestingly parallel-laid mats exhibited lower overall permeability than cross-laid mats compacted under the same pressure, due to fibre nesting and consequently lower porosity in parallel-laid mats.

Aligned reinforcements, such as nonwoven and woven fabrics, tend to produce anisotropic flow due to anisotropic permeability. The permeability anisotropy ratio of plain-woven jute fabric has been estimated to be 1.24 (Francucci et al. 2013).

#### 4.3.1.4 Saturated and Unsaturated Permeability

For synthetic reinforcements, ratios of saturated to unsaturated permeability ( $K_{\text{sat}}/K_{\text{unsat}}$ ) have been found to be greater than one, less than one or varying slightly above one (Dungan and Sastry 2002). Various reasons are proposed in literature for the observed result, including (1) flow channelling or fluid flow in preferential high-porosity regions (leading to  $K_{\text{sat}} > K_{\text{unsat}}$ ), (2) capillary and wicking effects (leading to  $K_{\text{unsat}} > K_{\text{sat}}$ ) and (3) transverse micro-flow into tows, which occurs after macro-flow between tows and increases penetration/impregnation times (leading to  $K_{\text{sat}} > K_{\text{unsat}}$ ) (Dungan and Sastry 2002).

It has been observed for natural fibre reinforcements that saturated permeability is higher than the unsaturated permeability.  $K_{\text{sat}}/K_{\text{unsat}}$  ranges between 1.2 and 1.8 for plain-woven jute fabrics (Dungan and Sastry 2002). Like Pillai and Advani (1998) and Dungan and Sastry (2002) argue that the jute yarns act as a ‘sink’, leading to a delayed impregnation of the tows through transverse micro-flow, which reduces the average macro-flow velocity, thereby reducing permeability.

An alternate explanation was provided for the high saturated permeability related to the absorption of fluid by the natural reinforcements (Dungan and Sastry 2002). Again, as the jute fibres and yarns act as sink components (as fibres absorb liquid, and yarns have micropores), the unsaturated permeability is reduced. Once infusion is complete (i.e. no more porosity within tows need to be filled and fibres cannot absorb more fluid), the fibres and yarns are no longer sink components, and the permeability upon saturation is increased. Note that the swelling of the fibres upon saturation does restrict flow paths and therefore the increase is only marginal. This argument is further strengthened by the fact that the difference between saturated and unsaturated permeability vanishes with increasing porosity (decreasing fibre volume fraction) (Fig. 4.11). In fact, at very high porosity ( $\phi > 0.8$ ),  $K_{\text{sat}}/K_{\text{unsat}} < 1$  (Fig. 4.11).

Notably, the difference between saturated and unsaturated permeability is higher in untreated jute fabrics ( $K_{\text{sat}}/K_{\text{unsat}} = 1.70\text{--}1.84$ ) than in treated jute fabrics ( $K_{\text{sat}}/K_{\text{unsat}} = 1.21\text{--}1.40$ ) (Dungan and Sastry 2002). This suggests that while transverse micro-flow into tows may play an important role in the difference in saturated and unsaturated permeability of natural fibre reinforcements, the polar nature of untreated natural fibres and their tendency to absorb polar fluids and swell have a more dominant role.

#### 4.3.1.5 Capillary Effects and Micro-Flow Versus Macro-Flow

Preform impregnation usually involves a dual-scale flow. Resin flow between yarns (inter-yarn) is referred to as macro-flow, while resin flow through the yarns (intra-yarn) is referred to as micro-flow. As resin flows at low Reynolds numbers, inertial

forces can be neglected. Macro-flow is dominated by viscous flow of the resin, while micro-flow is driven by capillary pressure developed within the tows. Capillary effects are important to study, not least because they play a key role in the mechanism of void formation in LCM. As Fig. 4.9 highlights, at low flow velocities (and high fibre volume fractions), capillary flow dominates leading to inter-yarn voids, while at high flow velocities (and low fibre volume fractions), viscous flow dominates leading to intra-yarn voids. This has been shown for plant fibre composites as well (Fig. 4.9) (Shah et al. 2012b; Shah 2013a).

Capillary effects in natural fibre reinforcements have received some attention (Francucci et al. 2012b; Sun et al. 2014), particularly due to the common (but incorrect) notion that the hollow structure of plant fibres may enhance capillary effects. There is little evidence that resin can impregnate the lumen, and in most cases the lumen has shown to remain unfilled after composite manufacture (Madsen 2004; Shah 2013a). Investigations have revealed that the dynamic capillary pressure in plain-woven jute fabrics was  $-25$  and  $36$  kPa when measured in the glycerine solution and vinylester resin, respectively (Francucci et al. 2012b). That is, spontaneous infiltration occurs during infusion with glycerine solution, but capillary forces act against flow during infusion with the resin. This has significant implications on experimental mould-filling tests as test fluids like glycerine solution may provide deceptively higher permeability and lower fill times.

The capillary pressure is found to increase exponentially with fibre volume fraction (Francucci et al. 2012b). Notably, the jute fabrics consistently exhibited capillary pressures two to three times higher than synthetic reinforcements (Francucci et al. 2012b), implying that capillary effects and micro-flow are more dominant in natural fibre reinforcements. Francucci et al. (2012b) also demonstrate that the measured capillary pressure may be used to determine a corrected unsaturated permeability, which is found to be similar for both the test fluid and resin.

## 4.3.2 Flow Modelling of Natural Fibre Composites

### 4.3.2.1 Introduction

Darcy's law (Eq. 4.11) and the continuity equation (Eq. 4.12) are commonly and conveniently used to describe the flow of thermosetting resins in porous reinforcements.

$$\bar{\mathbf{v}} = -\frac{K}{\mu} \nabla P, \quad (4.11)$$

$$\nabla \cdot \bar{\mathbf{v}} = 0, \quad (4.12)$$

where  $\bar{\mathbf{v}}$  is the volume-averaged fluid velocity and  $\nabla P$  is the applied pressure gradient.

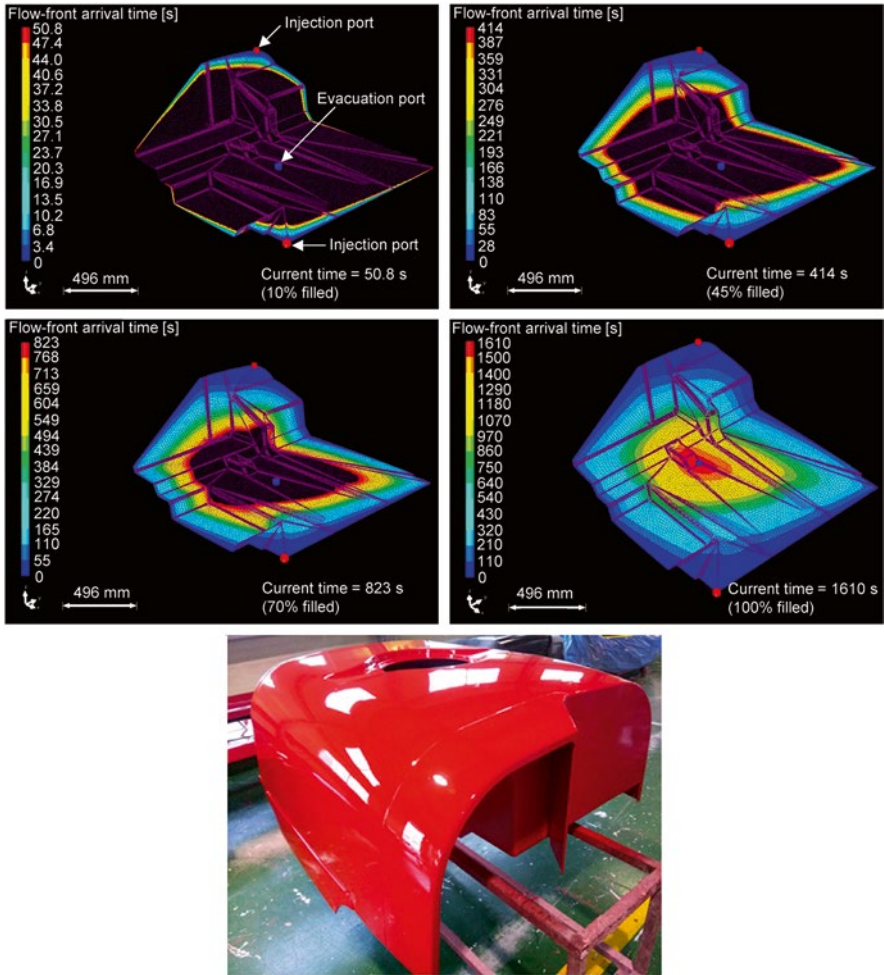


**Fig. 4.14** Resin flow simulation conducted in RTM-Worx software for the vacuum-assisted, light-RTM manufacture of the lower part of a flax/vinylester composite agricultural chemical storage tank. Adapted from Kong et al. (2014)

All permeability studies on natural fibre reinforcements so far have been conducted on the presumption of a valid 1D Darcy's law. The mould filling of natural fibre reinforcements has been successfully simulated and experimentally validated using the conventional model by some researchers, including Kong et al. (2014). They performed a resin flow analysis on the upper and lower parts of a flax/vinylester agricultural chemical storage tank, to predict fill times (and select a suitable injection pressure) and ensure complete impregnation. A flow simulation of the lower part is illustrated in Fig. 4.14. The simulations were backed by experiments.

### 4.3.2.2 Models Suitable for Natural Fibre Reinforcements

During resin impregnation in an LCM process, natural fibre reinforcements, unlike synthetic reinforcements, absorb liquid and subsequently swell. As discussed previously, the percentage absorption and swelling is dependent on the (polarity of the) liquid; for instance, jute swells by 18–22 % in glycerine solution but by 7–8 % in vinyl ester or polyester resin (Francucci et al. 2010). Due to the absorption of liquid, natural fibre preforms effectively act as a ‘sink’, soaking up some volume of the resin that is infused. The subsequent fibre volume change due to swelling has a twofold, time-dependent, ‘source-like’ effect: (1) reducing porosity and thus permeability and (2) increasing flow resistance. The conventional model in Eqs. (4.11) and (4.12) is therefore inappropriate, if not ineffective, in describing the permeability of, and resin flow behaviour in, natural fibre reinforcements as it does not take these sink and source factors into account.

Several researchers have recently attempted to develop flow models specifically for natural fibre reinforcements, including Languri et al. (2010), Nguyen et al. (2014), Masoodi et al. (2009), Masoodi and Pillai (2010, 2011) and Francucci et al. (2014). A modified continuity equation (Eq. 4.13) was initially proposed, which incorporated a sink term  $S(t)$  that was related to the rate of fluid absorption by the reinforcement and a porosity term  $\phi'(t)$  that was related to the rate of decrease in preform porosity due to increase in fibre volume upon swelling, both of which were functions of time (Languri et al. 2010; Masoodi et al. 2009; Masoodi and Pillai 2010, 2011). However, it was later found that sink and porosity terms had to cancel out to satisfy experimental observations (Masoodi and Pillai 2010, 2011); that is, the rate of fluid absorption (per unit volume) had to be equal to the rate of change of fibre volume (per unit volume). Consequently, Eq. (4.13) simplified to the conventional continuity equation of Eq. (4.12).

$$\nabla \cdot \bar{v} = -S(t) - \phi'(t). \quad (4.13)$$

Following this, Masoodi and Pillai (2011) proposed that the permeability  $K$ , alongside porosity  $\phi$  and fibre diameter  $d$ , were only functions of time (Eq. 4.14), where the subscript 0 indicates initial values (at  $t=0$ ). Essentially, if the change in fibre diameter over time (due to swelling) was measured, fitted curves could be used to then predict the evolution of porosity with time and the evolution of permeability with time. Then, if the evolution of the pressure gradient as a function of time was known, Eq. (4.15), which is derived by resolving Darcy’s law (Eq. 4.11) with the continuity equation (Eq. 4.13), could be used to predict the evolution of the flow front.

$$K(t) = \frac{\phi(t)^{n+1}}{C(1-\phi(t))^n}, \quad \text{where } \phi(t) = 1 - (1-\phi_0)\frac{d(t)}{d_0},$$

$$\text{and } d(t) = a \exp\left(\frac{b}{c+t}\right), \quad (4.14)$$

$$x^2(t) = \frac{2}{\phi_0 \mu} \int_0^t \Delta P(t) K(t) dt. \quad (4.15)$$

The above model has been used with much success by Masoodi et al. (2009), Masoodi and Pillai (2011) and Languri et al. (2010) in predicting the flow in natural fibre reinforcements. This particularly demonstrates the importance of tracking the evolution of permeability as a function of time in natural fibre reinforcements.

### 4.3.3 Conclusions

Permeability studies and data are imperative to understanding and modelling the mould-filling stage in LCM of composites. Plant fibre reinforcements demonstrate higher permeability than glass fibre reinforcements, while wood fibre reinforcements exhibit lower permeability than the latter. Permeability of natural fibre reinforcements increases with porosity and can be modelled by conventional models such as the modified Carman–Kozeny equation. Yarn diameter (linear density), length and twist level are all found to affect preform permeability. Fluid absorption and swelling are key mechanisms in natural fibre preforms, due to which both saturated and unsaturated permeability are reduced.

For natural preforms, saturated permeability tends to be higher than unsaturated permeability, although the difference vanishes with increasing porosity (decreasing fibre volume fraction). Moreover, capillary effects and micro-flow are more dominant in natural fibre reinforcements than in conventional synthetic reinforcements. Importantly, as natural fibres behave differently with different liquids (viz., absorption, swelling and capillary pressure), to accurately measure their permeability, the natural fibre reinforcement should be studied with the particular resin that is to be used during LCM as the test fluid.

To accurately model the mould-filling stage in LCM of natural fibre reinforcements, researchers have proposed experimentally validated Darcy's law-based models, which specifically incorporate effects of liquid absorption and subsequent fibre swelling on preform porosity and permeability as a function of time.

## References

- (18/06/2012). Samsara 'eco surfboard' features Biotex flax fibre. Retrieved 11/08/2014, from <http://www.reinforcedplastics.com/view/26369/samsara-eco-surfboard-features-biotex-flax-fibre/>
- Cai Z (1992) Analysis of mold filling in RTM process. *J Compos Mater* 26:1310–1338
- Campbell F (2003) *Manufacturing processes for advanced composites*. Elsevier, Oxford
- Carman P (1937) Fluid flow through granular beds. *Trans Inst Chem Eng Lond* 15:150–166
- Carus M (2011) Bio-composites: technologies, applications and markets. In: 4th international conference on sustainable materials, polymers and composites, Birmingham



- Carus M, Gahle C (2008) Natural fibre reinforced plastics – material with future. nova-Institut GmbH, Huerth
- Carus M, Eder A, Dammer L, Korte H, Scholz L, Essel R, Breitmayer E (2014) Wood-plastic composites (WPC) and natural fibre composites (NFC): European and global Markets 2012 and future trends. WPC/NFC Market Study 2014-03. nova-Institut GmbH, Hürth
- Chen B, Chou TW (1999) Compaction of woven-fabric preforms in liquid composite molding processes: single-layer deformation. *Compos Sci Technol* 59:1519–1526
- Chen B, Chou TW (2000) Compaction of woven-fabric preforms: nesting and multi-layer deformation. *Compos Sci Technol* 60:2223–2231
- Chen B, Lang EJ, Chou TW (2001) Experimental and theoretical studies of fabric compaction behavior in resin transfer molding. *Mater Sci Eng A* 317(1–2):188–196
- Correia N, Robitaille F, Long AC, Rudd CD, Simacek P, Advani SG (2005) Analysis of the vacuum infusion moulding process: I. Analytical formulation. *Compos A: Appl Sci Manuf* 36:1645–1656
- Duflou J, Deng Y, Acker KV, Dewulf W (2012) Do fiber-reinforced polymer composites provide environmentally benign alternatives? A life-cycle-assessment-based study. *MRS Bull* 37:374–382
- Dungan F, Sastry AM (2002) Saturated and unsaturated polymer flows: microphenomena and modeling. *J Compos Mater* 36(13):1581–1603
- Faruk O, Bledzki AK, Fink HP, Sain M (2012) Biocomposites reinforced with natural fibres: 2000–2010. *Prog Polym Sci* 37(11):1552–1596
- Francucci G, Rodriguez ES, Vazquez A (2010) Study of saturated and unsaturated permeability in natural fiber fabrics. *Compos A: Appl Sci Manuf* 41:16–21
- Francucci G, Rodriguez ES, Vazquez A (2012a) Experimental study of the compaction response of jute fabrics in liquid composite molding processes. *J Compos Mater* 46(2):155–167
- Francucci G, Vazquez A, Ruiz E, Rodriguez ES (2012b) Capillary effects in vacuum-assisted resin transfer molding with natural fibers. *Polym Compos* 33:1593–1602
- Francucci G, Vazquez A, Rodriguez ES (2013) Key differences on the compaction response of natural and glass fiber preforms in liquid composite molding. *Text Res J* 82(17):1774–1785
- Francucci G, Rodriguez ES, Moran J (2014) Novel approach for mold filling simulation of the processing of natural fiber reinforced composites by resin transfer molding. *J Compos Mater* 48(2):191–200
- Gassan J, Chate A, Bledzki AK (2001) Calculation of elastic properties of natural fibers. *J Mater Sci* 36:3715–3720
- Gauvin R, Kerachni A, Fisa B (1994) Variation of mat surface density and its effect on permeability evaluation for RTM modelling. *J Reinf Plast Compos* 13:371–383
- Goutianos S, Peijs T (2003) The optimisation of flax fibre yarns for the development of high-performance natural fibre composites. *Adv Compos Lett* 12(6):237–241
- Goutianos S, Peijs T, Nystrom B, Skrifvars M (2007) Textile reinforcements based on aligned flax fibres for structural composites. In: *Composites innovation 2007 – improved sustainability and environmental performance*, Barcelona
- Gutowski T, Cai Z, Bauer S, Boucher D, Kingery J, Wineman S (1987a) Consolidation experiments for laminate composites. *J Compos Mater* 21:650–669
- Gutowski T, Morigaki T, Cai Z (1987b) The consolidation of laminate composites. *J Compos Mater* 21:172–188
- Ho M, Wang H, Lee J, Hoc C, Lau K, Leng J, Hui D (2012) Critical factors on manufacturing processes of natural fibre composites. *Compos Part B* 43(8):3549–3562
- Kelly P, Umer R, Bickerton S (2004) Compaction of dry and wet fibrous materials during infusion processes. In: *36th international SAMPE technical conference*, vol 36. San Diego, pp 785–797
- Kim Y, McCarthy SP, Fanucci JP (1991) Compressibility and relaxation of fiber reinforcements during composite processing. *Polym Compos* 12(1):13–19
- Ko F, Kawabata S, Inoue M, Niwa M, Fossey S, Song JW (2001) Engineering properties of spider silk. In: *MRS proceedings*. vol 702. doi:[10.1557/PROC-702-U1.4.1](https://doi.org/10.1557/PROC-702-U1.4.1)

- Kong C, Park H, Lee H, Lee J (2014) Design of natural fiber composites chemical container using resin flow simulation of VARTML process. *Int J Mater Mech Manuf* 2(3):256–260
- Languri E, Moore RD, Masoodi R, Pillai KM, Sabo R (2010) An approach to model resin flow through swelling porous media made of natural fibers. In: 10th international conference on flow processes in composite materials (FPCM10), Monte Verità, Ascona
- Lewin M (2007) *Handbook of fiber chemistry*. CRC Press LLC, Boca Raton
- Li Y (2006) Processing of sisal fiber reinforced composites by resin transfer molding. *Mater Manuf Process* 21(2):181–190
- Long A, Boisse P, Robitaille F (2005) Mechanical analysis of textiles. In: Long A (ed) *Design and manufacture of textile composites*. Woodhead Publishing Limited and CRC Press LLC, Cambridge
- Lundquist L, Willi F, Leterrier Y, Manson JAE (2004) Compression behavior of pulp fiber networks. *Polym Eng Sci* 44(1):45–55
- Madsen B (2004) *Properties of plant fibre yarn polymer composites – an experimental study*. PhD, Technical University of Denmark
- Manson J, Wakeman MD, Bernet N (2000) 2.16 – Composite processing and manufacturing – an overview. In: Kelly A, Zweben CH (eds) *Comprehensive composite materials*. Pergamon & Elsevier Science, Oxford (vol 2, Polymer matrix composites)
- Masoodi R, Pillai KM (2010) Darcy's law-based model for wicking in paper-like swelling porous media. *Am Inst Chem Eng J* 56(9):2257–2267
- Masoodi R, Pillai KM (2011) 3 – Modeling the processing of natural fiber composites made using liquid composite molding. In: Pilla S (ed) *Handbook of bioplastics and biocomposites engineering applications*. Wiley, Hoboken
- Masoodi R, Pillai KM, Verhagen MA (2009) Flow modeling in natural-fiber preforms used in liquid composite molding. In: *Joint American-Canadian international conference on composites*, Newark
- Matsudaira M (2006) Fabric handle and its basic mechanical properties. *J Text Eng* 52(1):1–8
- Matsudaira M, Qin H (1995) Features and mechanical parameters of a fabric's compressional property. *J Text Inst* 86(3):476–486
- Neuman S (1977) Theoretical derivation of Darcy's law. *Acta Mech* 25:153–170
- Nguyen V, Lagardère M, Cosson B, Park CH (2014) Experimental analysis of flow behavior in the flax fiber reinforcement with double scale porosity. In: 12th international conference on flow processing in composite materials (FPCM 12), Enschede
- Parnas R, Howard JG, Luce TL, Advani SG (1995) Permeability characterization. Part 1: a proposed standard reference fabric for permeability. *Polym Compos* 16(6):429–445
- Pickering K (ed) (2008) *Properties and performance of natural-fibre composites*. CRC Press LLC, Boca Raton
- Pillai K, Advani G (1998) A model for unsaturated flow in woven fiber preforms during mold filling in resin transfer molding. *J Compos Mater* 32(19):1753–1783
- Placet V, Trivaudey F, Cisse O, Gucheret-Retel V, Boubakar ML (2012) Diameter dependence of the apparent tensile modulus of hemp fibres: a morphological, structural or ultrastructural effect? *Compos A: Appl Sci Manuf* 43(2):275–287
- Reux F (2012) Worldwide composites market: main trends of the composites industry. In: 5th innovative composites summit – JEC ASIA 2012, Singapore
- Richardson M, Zhang ZY (2000) Experimental investigation and flow visualisation of the resin transfer mould filling process for non-woven hemp reinforced phenolic composites. *Compos A: Appl Sci Manuf* 31:1303–1310
- Robitaille F, Gauvin R (1998a) Compaction of textile reinforcements for composites manufacturing. I: review of experimental results. *Polym Compos* 19(2):198–216
- Robitaille F, Gauvin R (1998b) Compaction of textile reinforcements for composites manufacturing. III: reorganization of the fiber network. *Polym Compos* 20(1):48–61
- Rodriguez E, Giacomelli F, Vazquez A (2004) Permeability-porosity relationship in RTM for different fiberglass and natural reinforcements. *J Compos Mater* 38:259–268

- Rodríguez E, Stefani PM, Vazquez A (2007) Effects of fibers' alkali treatment on the resin transfer molding processing and mechanical properties of jute-vinylester composites. *J Compos Mater* 41:1729–1741
- Schiefer H (1933) The compressometer, an instrument for evaluating the thickness, compressibility, and compressional resilience of textiles and similar materials. *Bur Stand J Res* 10(6):705–713
- Shah D (2013a) Characterisation and optimisation of the mechanical performance of plant fibre composites for structural applications. PhD, University of Nottingham
- Shah D (2013b) Developing plant fibre composites for structural applications by optimising composite parameters: a critical review. *J Mater Sci* 48(18):6083–6107
- Shah D, Schubel PJ, Clifford MJ, Licence P (2011) Mechanical characterization of vacuum infused thermoset matrix composites reinforced with aligned hydroxyethylcellulose sized plant bast fibre yarns. In: 4th international conference on sustainable materials, polymers and composites, Birmingham
- Shah D, Schubel PJ, Clifford MJ, Licence P (2012a) The tensile behavior of off-axis loaded plant fiber composites: an insight on the non-linear stress–strain response. *Polym Compos* 33(9):1494–1504
- Shah D, Schubel PJ, Licence P, Clifford MJ (2012b) Determining the minimum, critical and maximum fibre content for twisted yarn reinforced plant fibre composites. *Compos Sci Technol* 72:1909–1917
- Shah D, Schubel PJ, Clifford MJ (2013a) Can flax replace E-glass in structural composites? A small wind turbine blade case study. *Compos Part B* 52:172–181
- Shah D, Schubel PJ, Clifford MJ (2013b) Modelling the effect of yarn twist on the tensile strength of unidirectional plant fibre yarn composites. *J Compos Mater* 47(4):425–436
- Shah D, Schubel PJ, Clifford MJ, Licence P (2013c) Mechanical property characterization of aligned plant yarn reinforced thermoset matrix composites manufactured via vacuum infusion. *Polym Plast Technol Eng* 53(3):239–253. doi:10.1080/03602559.2013.843710
- Shah D, Porter D, Vollrath F (2014a) Opportunities for silk textiles in reinforced biocomposites: studying through-thickness compaction behaviour. *Compos A: Appl Sci Manuf* 62:1–10
- Shah D, Schubel PJ, Clifford MJ, Licence P (2014b) Mechanical property characterization of aligned plant yarn reinforced thermoset matrix composites manufactured via vacuum infusion. *Polym Plast Technol Eng* 53:239–253
- Summerscales J, Dissanayake N, Virk AS, Hall W (2010) A review of bast fibres and their composites. Part 2 – composites. *Compos A: Appl Sci Manuf* 41(10):1336–1344
- Sun Z, Zhao X, Ma J (2014) Capillary effect in the impregnation of jute fiber mat reinforced polypropylene composites. *J Compos Mater* 48:447–453
- Umer R, Bickerton S, Fernyhough A (2007) Characterising wood fibre mats as reinforcements for liquid composite moulding processes. *Compos Part A* 38:43–448
- Umer R, Bickerton S, Fernyhough A (2008) Modelling the application of wood fibre reinforcements within liquid composite moulding processes. *Compos Part A* 39:624–639
- Umer R, Bickerton S, Fernyhough A (2011) The effect of yarn length and diameter on permeability and compaction response of flax fibre mats. *Compos A: Appl Sci Manuf* 42:723–732
- van Wyk C (1946) 20 – Note on the compressibility of wool. *J Text Inst Trans* 37(12): T285–T292
- Winson C (1932) 27 – Report on a method for measuring the resilience of wool. *J Text Inst Trans* 23(12):T386–T393
- Witten E, Jahn B (2013) Composites market report 2013: market developments, trends, challenges and opportunities. *Industrievereinigung Verstärkte Kunststoffe (Federation of Reinforced Plastics) and Carbon Composites eV, Frankfurt*
- Xue D, Miao M, Hu H (2011) Permeability anisotropy of flax nonwoven mats in vacuum-assisted resin transfer molding. *J Text Inst* 102(7):612–620
- Yang J, Xiao J, Zeng J, Jiang D, Peng C (2012) Compaction behavior and part thickness variation in vacuum infusion molding process. *Appl Compos Mater* 19:443–458
- Zhang K, Si FW, Duan HL, Wang J (2010) Microstructures and mechanical properties of silks of silkworm and honeybee. *Acta Biomater* 6:2165–2171